UNITED STATES

DEPARTMENT OF THE INTERIOR

GEOLOGICAL SURVEY

INTERAGENCY REPORT NASA-123

AERIAL INFRARED SURVEYS AT THE GEYSERS GEOTHERMAL STEAM FIELD, CALIFORNIA*

by

R. M. Moxham**

Prepared by the Geological Survey
for the National Aeronautics and
Space Administration (NASA)

*Work performed under NASA Task No. 160-75-01-53-10, Work Order T-65754-G
**U.S. Geological Survey, Washington, D.C.

CONTENTS

TABLE

ILLUSTRATIONS

Rocks are poor conductors of heat. Even in regions where the geothermal flux is 100 times normal (normal being $\sim 1.5 \times 10^{-6}$ cal cm^{-2} sec^{-1}) the outward heat flow from the earth is 50 times less than the incoming solar flux. Considering the added local variations in the surface thermal regime stemming from meteorological factors, the slight increase in heat flux from a subsurface source would likely be concealed in the noise. Heat transfer by convection however, gives rise to obviously abnormal surface temperatures where liquids and gases transfer heat to rocks along their path. Consequently, convective heat transfer seems most likely involved in any detectable surface temperature anomaly and direct detection of the underground source due to upward heat conduction is not very likely.

GEOLOGIC SETTING

The Geysers area is in Sonoma County, about 70 miles NNW of San Francisco. Relief is relatively rugged for our purposes, amounting to some 1,500 feet, with steep valley walls so that it was not possible to fly as low as desired over some of the area (fig. 2).

Most of the report area is included in a 1:62,500 scale geologic map by Bailey (1946). The area in the vicinity of the steam field has been mapped on a larger scale by McNitt (1963) (fig. 3), with some revisions in 1965. A detailed study of the fumaroles and hot springs is given in the excellent work of Allen and Day (1927). We have used these works extensively in the accompanying geologic descriptions and maps.

Figure 3 shows a portion of The Geysers area as mapped by McNitt. It is underlain by the Franciscan Formation (Jurassic-Cretaceous) which consists of the following, from base upward: massive graywacke, with minor amounts of shale (JKs); several hundred feet of greenstone (gs) with associated chert beds and with serpentinized peridotite (sp) at the upper and lower contacts; and poorly bedded micaceous graywacke and shale (JKms).

Cobb Mountain near the northeast corner of the report area is capped by rhyolite and other effusive rocks which Bailey (1946), citing earlier work, relates to the Sonoma volcanics of Pliocene age. During Pleistocene time, extensive eruptions occurred northeast of the Mayacamas Mountains, forming the Clear Lake volcanic field that extends within 5 miles of the report area. No Tertiary or Quaternary volcanic rocks have been found at depth in The Geysers area.

The regional grain of the Franciscan rocks of the Mayacamas Mountains is northwesterly, stemming from a series of faulted structural blocks bounded by steeply-dipping arcuate faults, according to McNitt's interpretation (fig. 3). Vertical displacement is estimated to be at least 2,000 feet on one fault block, but total displacement on the major fault systems is doubtlessly much larger. The Geysers area is on the northeast side of a down-thrown block, flanked on the northeast by the Cobb Mountain horst.

A linear zone of hydrothermal activity extending for perhaps 25 miles and including The Geysers, was recognized early in the exploration for quicksilver (Allen and Day, 1927, p. 11). The alinement, which parallels the regional northwesterly strike, contains at intervals, hot springs, fumaroles and zones of hydrothermal alteration. The principal hot springs in the report area are accociated with the hydrothermal alteration zones shown on figure 2. For a detailed description of the springs and fumaroles, see Allen and Day (1927). The most important hot spring activity is in Geyser Canyon, from its mouth at Big Sulphur Creek and extending up the canyon for several hundred yards. Most of the springs are above 60°C and several are at the boiling point. The highest fumarole temperature reported by Allen and Day (1927, p. 25) in The Geysers area was 102°C at the "Safety Valve" in Geyser Canyon.

Another fumarole field, the Sulphur Banks, is about one mile west of Geyser Canyon. It is also characterized by soft, steaming ground where temperatures at the numerous gas vents are in the 90°C range.

Upstream from The Geysers resort, several hot springs are found in the valley of Big Sulphur Creek and on Hot Springs Creek. At the Little Geysers, a group of hot springs in the 80°-95°C range occurs in a barren alteration zone.

Based on the Day and Allen measurements, McNitt assumes the total natural thermal spring discharge to be 5,000 gal/hr., representing a minimum natural heat loss of about 4.2×10^5 cal/sec. This amount does not include losses by evaporation and radiation.

Drilling for steam by the Magma and the Thermal Power Companies began in 1955 in the Geyser Canyon alteration zone. Superheated steam was produced from depths of 500 to 1,200 feet. Development at this locale continued and drilling later was extended westward to the Sulphur Banks (fig. 3) where deeper steam production was found at pressures to 500 psi. At present (December, 1967), forty-two wells have been drilled from 1,500 to 6,000 feet deep in an area of about 300 acres. The amount of steam on line and proved by drilling is capable of producing on the order of 200 megawatts (McNitt, oral comm.). Since 1967, Union Oil Company has undertaken drilling here in partnership with Magma Thermal Power Company.

Several wells have been drilled that lie beyond the present productive area. Those that are generally regarded as successful are designated "S" in the following remarks. The remainder are either listed in State reports as plugged and abandoned, or are generally understood not to meet present commercial requirements. The last entry had not been completed at the time this report was written.

Location	Destination on fig. 2	Well designation	Remarks
Sec. 12,T11N,R9W	G	Union Oil Co., Ottobani no. 1	S
Sec. 14,T11N,R9W	E	Geothermal Resources Inc., no. 1	S
Sec. 14,T11N,R9W	F	Geothermal Resources Inc., no. 2	S
Sec. 18,T11N,R8W	D	Signal Oil Co., Cobb Mtn., no. 1	S
Sec. 33,T11N,R8W	K	Little Geysers no. 1	S
Sec. 28,T11N,R8W	H	Geysers Development Co., 65-28	S
Sec. 35,T12N,R9W	C	Signal Oil Company Wild Horse no. 1	
Sec. 10,T11N,R9W	A	Signal Oil Company Wild Horse no. 2	
Sec. 28,T11N,R8W	J	Little Geysers no. 2	
Sec. 33,T11N,R8W	L	D and V 73-33	Drilling, 9/68

Based upon these developments, Otte and Dondanville (1968) state that a 600,000 KW power potential for the area may be conservative.

Temperature-depth measurements were made in 1960 in eight steam wells of the Thermal Power Company. In each, a constant temperature interval was recorded in the upper part of the well, which McNitt (1967, p. 18) suggests is caused by groundwater overlying the steam reservoir. Further, hydrostatic equilibrium exists between the two phases whereby the expansive pressure of the steam is balanced by the hydrostatic pressure of the overlying water body. Calculation of the hydrostatic head leads to the conclusion that the steam-water interface slopes roughly parallel to the topographic surface in this vicinity.

EQUIPMENT AND TECHNIQUES

The aerial infrared equipment used in this survey was a conventional line scanner. The terrain is scanned along a line normal to the flight path by means of a rotating 45° mirror. The infrared emission from the earth is reflected through the optical system onto a solid state detector. The detecting element converts the optical signal to electrical form which, after amplification, modulates a light source focused on a film strip. The light source is deflected across the film in synchronization with the scanning mirror, and the film strip advances in proportion to the aircraft velocity. This combined light deflection and film motion thus creates an image whose gray scale is related to the infrared energy emitted from the terrain. The line scanner used in this work is not a radiometer, however. That is, the scanner output signal (and therefore the image tone) is not a direct measure of the incoming infrared energy, owing mainly to the AC characteristics of the amplifiers. This matter will be dealt with below.

The scanner was equipped with an electrically-cooled Ge:Hg detector having maximum response in the 8-14 micrometer (μm) region. Narrow band pass dielectric filters were placed in the optical path to limit the detector response on selected flights.

The scanner was carried in a twin-engine D-18 Beechcraft operated by the USGS Water Resources Division. Portable rotating beacons were placed at strategic locations on ridge tops to assist night navigation.

During the survey period, temperatures of water and soil were monitored at selected localities. Yellow Springs Instrument Company Series 400 thermistors were employed. At each site, thermistors were

emplanted a 2 or 3 mm below the surface in the soil or in a rock crack. For water temperatures, the thermistors were attached to floats in such a way that the elements were submerged a few centimeters. The thermistor resistance was measured with an automatic sequencing bridge and the results were recorded on an Esterline-Angus strip chart recorder. The temperature monitoring equipment is described in detail elsewhere (Moxham and others, 1968).

The film produced by the scanner is a conventional negative so that higher terrain radiance produces darker image tones i.e., greater film density. Consequently, where we have occasion in this report to refer to film density, higher densities refer to higher terrain radiance. All images accompanying this report are positive prints from the original negative, hence, whiter tones correspond to higher terrain radiance; darker tones correspond to lower terrain radiance.

AERIAL SURVEYS

Aerial surveys were made during August 15-19, 1966. Nine lines about four miles long and spaced at about one mile intervals were flown NNE, approximately normal to Big Sulphur Creek valley. This grid was centered on the steam-producing area. Another line was flown WNW, along Big Sulphur Creek from about the Sonoma-Lake County line to Squaw Creek.

One afternoon IR flight was made, using an 8-14μm band pass filter over the detector. All other IR surveys were made from 02:30-05:00, with the detector open (unfiltered) or with 8-14, 8.9-10 and 10-15μm filters.

Several flights were made over Clear Lake, 10 miles NE of The Geysers, to provide additional targets whose temperatures could be readily monitored. A temperature monitoring station was established on the west shore of the lake, about one mile northwest of Fraser Point.

Aerial panchromatic 70mm photographs along the survey lines were made on one flight.

It is a matter of some interest in aerial IR surveying to know the time at which the onset of solar heating at sunrise will begin to have a detectable effect on surface temperature. The first light of dawn is sometimes desirable, if not mandatory for low level aerial navigation over rugged terrain. But as the sun rises, the surface temperature at some point in time begins to increase and to obscure thermal features one desires to depict. We have shown elsewhere (Moxham and others, 1968, p. 9) that there is roughly a one hour lag between first light of dawn and the onset of surface heating at sunrise (figure 4). Surface temperature begins to rise just a few minutes after sunrise.

DATA ANALYSIS

Problems in data analysis center on geometrical and electrical sources of error and upon several other uncertainties. Inspection of nearly any of the IR images accompanying this report with respect to the planimetry in figure 2, is sufficient to demonstrate the geometric distortion common to most of the present generation of scanners. Where landmarks are well resolved and in the case where one is only interested in image density, the distortion may be of minimum consequence. Where few landmarks can be identified, image distortion makes it very difficult to locate geographically a particular point on the image and it is nearly impossible to superpose the image on a photo or map, for comparison with other data.

The well known relationship between terrain radiance and surface temperature have led some writers to quantitatively analyze IR image density in terms of surface temperature. This is a hazardous business at best, for several reasons. First, most IR scanners are not radiometers in that there is not a straightforward relationship between radiance at the entrance aperture and the output signal. This is largely a matter of the instrument's electrical characteristics.

Second, the recording system leaves much to be desired. Exposure of the recording film is not constant but rather is a function of the film speed through the transport system, which in turn depends on the surveying altitude. Moreover, variations in image tone can be produced by using films of different gammas and by film development processes. Third, the atmosphere both absorbs the terrain signal and emits its own energy, the new result depending upon wavelength, scan angle (ie., path length) and the temperatures of the two media.

No attempt has been made to evaluate these parameters individually in any rigorous way, but some film density analyses were made to examine some of the more evident sources of error.

Before discussing the results, a brief description of the film density analyzers will be useful.

Film density analyzers

A Joyce-Loebl microdensitometer-isodensitracer (MDT-IDT) and a Tech/Ops image quantizer were used to measure the IR film densities (for details on the operation and use of these instruments, see Turner and Boynton, 1968). Essentially, both instruments sense the density by means of a light beam passed through the film specimen onto a photocell. The IDT-MDT compares the light beam intensity with a reference beam passed through a standard density wedge. By moving the film in the Y direction, the MDT provides a density profile along the film; the IDT contours the density, using X and Y motion of the film carriage.

Accurate density measurement of a given feature on the imagery requires that the feature completely fill the aperture. To resolve small thermal features, a small aperture, say 50$^{\mu}$m, is desireable. But the small aperture also resolves high frequency noise. At larger apertures, say 400μm, the high frequency noise is diminished but with corresponding loss of detail in the terrain information. Low frequency components are retained in both instances as the wave length greatly exceeds any reasonable aperture setting. In practice, in the contouring mode particularly, we have found a 300μ aperture to be a useful compromise.

The Tech/Ops image quantizer light beam passes through the specimen film, which is rotated on a drum. The light intensity through the specimen modulates the voltage on a spark stylus which in turn prints the density contours on sensitized paper.

Several flights were made over Clear Lake and the adjacent shoreline with the IR detector "open" (unfiltered) and with 8-14, 8.9-10, and 10-15μm bandpass filters. Figure 5 shows one of the images and figures 6 and 7 are MDT profiles of the several image densities.

In figure 5, the Clear Lake portion of the image shows the fine lines (several per millimeter) parallel to scan direction, which are due to film drive jitter. These are sometimes referred to as scan lines, but they result from the slightly non-uniform motion of the IR recording film transport system in the scanner. The jitter lines give rise to high frequency "noise" in the MDT film density profile and is altitude (scale) independent. The noise amplitude is relatively inconsequential in face of the more formidable problems. For example, there are evident on figure 5 dark streaks in the lake (parallel to scan direction) which correlate with the low frequency variations on the density profile. The dark bands result from the scanner electronics. The scanner amplifiers are AC-coupled to achieve optimum high frequency response and therefore optimum small target resolution. The scanner prints out the signals, positive and negative, above and below an average DC level. Unfortunately, there is no clamping or DC level restoration so that the gray tone of the image is dependent upon the average DC level along the scan line. This effect is most pronounced where the incoming signal is nearly DC, e.g., from a large body of water of uniform temperature.

The lack of DC restoration is particularly evident on figure 6A, a density profile along the flight track over Clear Lake. The signal from Clear Lake is essentially DC, and occupies a large part of the scan line. But the signal from the adjacent shore line area varies locally so that the shore line signal level raises or lowers the average DC level, giving rise to

light and dark bands across the lake.

(In spite of this low frequency component, one can see in the lake irregular tonal patterns that no doubt represent real temperature variations. For example, there is a small, but distinct discharge of warm water from a boat basin just east of the flight line at station 4. A band of warmer water along the west shore is also faintly suggested; several faint oval-shaped patterns are seen elsewhere).

Figure 7 shows a series of profiles across the image, parallel to the scan direction. It is evident (e.g., fig. 7A) that there is a signal drop-off toward the horizons, probably due to atmospheric effects. The intervening atmosphere absorbs part of the terrain signal. As the atmospheric transmission decreases with path length, absorption of the terrain signal correspondingly increases as the scan angle sweeps from the vertical toward the horizon. At the same time the reverse effect operates, as the atmosphere itself emits along the scan path. However, from the data cited below, atmospheric absorption is evidently the more effective mechanism at the terrain and atmospheric temperatures encountered in these surveys.

The Ge:Hg detector is generally termed a "long wavelength" detector as it has peak sensitivity at about 10μm. However the sensitivity range extends well beyond the 8-13μm atmospheric window so that if no filter is used, as in figure 7A, noticeable atmospheric absorption will result from the water vapor bands adjacent to the 8-13μm window. Restricting the incoming signal to the more transparent parts of the 8-13μm window (figures 7B-D) tends to reduce the atmospheric losses but also reduces the effective temperature sensitivity.

Tri-X Aercon film was used in all of the surveys reported here. No special efforts were made to control the development although the processing followed a standard routine with respect to the chemicals and development time.

The effects of some of the foregoing sources of errors are summarized in figure 8. It suggests that an 8-14μm filter is probably the best compromise between atmospheric absorption and terrain signal loss. Though the limit of error for the 8-14μm band pass is only about 1°C, these data represent an ideal case. It is evident that with different land-water temperatures and geometry, the lack of DC restoration could introduce much larger errors. Moreover, no account has been taken here of the variations in film exposure and development and the effects of instrument parameters such as automatic gain control.

Diurnal temperature effects

One of the principal areas of interest is the present steam production site on the north side of the valley of Big Sulphur Creek. This rather steeply sloping surface is largely grass-covered with scattered trees. Along the drainages, trees and brush are more abundant (figure 9). The south valley slope, on the other hand, has a heavy growth of trees and brush. Figure 9 is an aerial photo taken in 1955 before the extensive cultural changes resulting from the drilling for steam. The picture shows rather well the light-colored barren patches of hydrothermal alteration against the darker background of the grass-covered unaltered ground. The same area photographed during our survey in August 1966, shows the extensive cultural changes that have taken place, but the Geyser Canyon alteration zone is not very well depicted (figure 10).

A daytime IR image of this area (fig. 11) shows only the highest surface temperatures in a doughnut-shaped pattern where copious steam is escaping around the drilling pad of a blown-out steam well. The shaded, cooler vegetation contrasts strongly with the hot, sun-lit grass-covered slope. Many of the topographic features on the IR resemble those on the aerial photo due to shadows that create differences in solar heating.

A pre-dawn image of the same area (fig. 12B), shows how the diurnal cooling effects the IR emission. The lower-temperature geothermal anomalies now contrast strongly against the cooler grassy slopes. The vegetation is apparently about at the same radiant temperature as the soil. Cooler air has settled into topographic lows, and with no filter over the detector, gives rise to the cooler surfaces in the basin of Big Sulphur Creek; dark mottling correlates with smaller topographic depressions.

The increase in temperature difference between anomaly and background from afternoon to pre-dawn is borne out by ground temperature measurements at the Sulphur Banks (fig. 13 and 14). Three thermistors were emplanted at random in a warm alteration zone at station 1. Another three-thermistor array was established at station 2 on a flat bare soil surface about 500 feet NW of the anomaly at station 1. The results (fig. 14) show that during the day the background is at about the same temperature as the anomaly, whereas in the pre-dawn hours the average temperature at the anomaly is about 10° greater than the background.

The bare soil at background station 2 appeared to be fairly uniform in texture and composition; the temperature spread among the three thermistors was on the order of 1.5°C. In the alteration zone, there is a much greater spread among the thermistors owing to the local percolation of warm gases through the soft ground, and perhaps to slight variations in depth of the thermistors.

Pre-dawn thermal emission

An over-all thermal view of the report area is shown in figure 15. Additional details are on figures 12 and 16. The most intense anomalies lie for the most part in the alteration zones shown in figure 2. The group of springs at the Little Geysers (fig. 16) is the southeastern-most prominent anomaly, though there seems to be a small unidentified hot spot about 1/4 mile further upstream on Big Sulphur Creek. Additional anomalies, apparently associated with hot springs, occur along Big Sulphur Creek between Little Geysers and powerhouse 1. The most prominent is about one mile SE of the mouth of Hot Springs Creek. The springs on Hot Springs Creek are barely perceptible, by contrast.

The two most intense anomalies lie between powerhouse 1 and Geyser Canyon. They are in the area's largest alteration zone and it is here that steam development first began. Natural steam vents at 90°C are common, and on the westernmost of the two anomalies steam from the cracked drilling pad of a wild-blowing well adds to the thermal signal. The southwest limit of the anomalous zone is a thermal lineament which extends along the north bank of Big Sulphur Creek from the powerhouse nearby to the mouth of Geyser Canyon. A similar WNW linear thermal zone lies along the creek from near the mouth of Geyser Canyon downstream along Big Sulphur Creek for several hundred yards. This zone likewise forms the southern limit of a zone of hot spots in the valley next west of Geyser Canyon. The image suggests and field examination tends to confirm that the linear thermal zone contains two steaming fracture zones, one about at creek level, the other 20 feet or so above the creek (fig. 17).

Further west the Sulphur Banks anomalies are in an area mantled by landslides. The hot patches form a 1/2 mile long line of interconnected thermal spots extending WNW from near powerhouse 2.

En echelon with the Sulfur Banks thermal zone, is a straight reach of Big Sulphur Creek along which are several small thermal spots; they are probably due to hot springs, as the creek brightness on the image is perceptibly higher along this reach.

It thus appears that the two most prominent mapped thermal zones are bounded on the south by linear features and a third is linear in shape. Though the thermal alignments do not coincide with any of the faults mapped by McNitt, an abnormally warm fracture system along parts of Big Sulphur Creek is strongly suggested.

The most intense thermal anomalies in The Geysers area coincide generally with hydrothermally altered steaming ground. IR maxima are recorded over active fumaroles and hot springs. But close inspection of figure 12C and figure 15 shows a subtle arcuate low intensity thermal feature extending northwest from the Sulphur Banks. To try to objectively evaluate this feature with respect to its environs and to the adjoining high intensity thermal anomalies, we employed the two density analyzers described previously.

The image quantizer was used as a film density level slicer. In this procedure, the specimen is scanned with the quantizer set so that it prints only those densities greater than a certain selected value. The process is then repeated, changing only the quantizer threshold so that it prints slightly lower densities. The process is repeated at successively lower thresholds, yielding a set of prints as in figure 18. The IR image used in this case was that shown in figure 12.

Figure 18 covers Big Sulphur Creek valley from about Hot Springs Creek to about one mile SE of the Buckeye Mine, and in figure 18A, depicts maximum film densities in this area. The highest density is in the main alteration zone at a point about midway between powerhouse 1 and Geyser Canyon. The hottest parts of the anomalies at the Sulphur Banks also fall in this density increment, including the site at station 1. The next lower density increment (18B) increases the size of the Geyser Canyon thermal zone by perhaps a factor of 2 and the Sulphur Banks zone by somewhat more. The alteration zone, about midway between Geyser Canyon and powerhouse 2, now makes its appearance rather faintly. But perhaps more significant is the development of an arcuate density zone extending west from the Sulphur Banks, and after a gap, an oval-shaped ring of density features still further to the west.

Adding the next lower density increment (figure 18C), there is essentially no further enlargement of the Sulphur Banks-Geyser Canyon suite of anomalies, but the area west of Sulphur Banks is greatly enlarged and several spots are included SE of The Geysers and south of Big Sulphur Creek.

The next added density increment prints out roughly half the area of the IR image.

It seems safe to say that figure 18A depicts only thermal anomalies, as all of the localities relate directly to steaming ground. At the other extreme, figure 18D must be well into the geologic noise level. This intuitive reasoning leads to the conclusion that the boundary between normal and abnormal surface temperatures ought to be at some intermediate density level between 18A and 18D.

An IR image of Big Sulphur Creek valley (fig. 12) was also analyzed with the IDT-MDT, with generally comparable results. The isodensity map is printed out with each density increment depicted by a separate color for ease of identification (see Turner and Boynton 1967, for details on the color attachment). The boundaries of the two maximum isodensity zones are shown on figure 20. Temperatures at ground stations 1 and 2 were recorded (fig. 14) at the time the image was made. Station 1 is within the anomaly; station 2 is just beyond. The observed 11°C average temperature difference between these stations gives some measure of the anomaly.

Another IR image of Big Sulphur Creek valley (fig. 15) on a smaller scale than figure 12 and covering a larger area, was also processed on the IDT-MDT. The density increments of figures 20 and 21 do not correspond precisely but the general distribution of maximum densities is similar in both instances. In December, 1967, soil temperature measurements were made in the area of higher radiance west of the Sulphur Banks. A linear array of 5 thermistors spaced at about 50 foot intervals was emplanted on the south-sloping ridge between two landslides in the SE 1/4 sec. 11, T11N R9W (fig. 13). The array was intended to cross the arcuate fault mapped here by McNitt (fig. 3). At most of the thermistor sites, the bedrock evidently was at shallow depth, on the order of inches. The results (fig. 22) indicate a nighttime difference of about 7°C between the two thermistors on the south as opposed to the three on the north. A direct comparison of this temperature break with the IR results would hardly be justified, owing to seasonal differences if nothing else, but it seems evident there is some anomalous soil temperature condition at

this locality. A good deal more surface observations would be required before one were to draw any further conclusions.

In the foregoing density analyses, unfiltered images were utilized to take advantage of the maximum signal response. By the same token, as previously demonstrated, the unfiltered images suffer the greatest atmospheric transmission losses, that reduce the apparent radiance toward the image edges. This effect is illustrated in figure 23, where the colder air in topographic depressions and the density roll-off with increased scan angle are much more evident on the unfiltered image than on the 8-14 band pass. The density maps consequently are useful only in comparing relative densities in the central part of the image and on a local basis.

From a regional standpoint, the radiance in the Big Sulphur Creek area shows no diagnostic character that we can identify. MDT density profiles were made of several IR images oriented NE that extend from Little Sulphur Creek to Squaw Creek. In all cases, radiance levels in Big Sulphur Creek valley do not exceed those in the adjacent areas except for the immediate vicinity of the hydrothermal zones (figures 24 and 25). The arcuate radiance zone west of the Sulphur Banks is visible on these regional images, but the absolute value of the radiance level is relatively low. The higher radiance levels elsewhere in the region can be ascribed locally to vegetation and to slope orientation with respect to sun angle, but there is not a great deal of consistency. Variation in emissivity may also be involved. Representative samples of several bedrock units in The Geysers area were examined with an emissivity box (Moxham and others 1968, p. 11) utilizing a Barnes 8-14μm radiometer. The results

Table 1. Emissivity (8-14mμ) of rocks in The Geysers area

Sample	Location	Description	$\bar{\varepsilon}$8-14
1	SW 1/4 sec. 11 T11N, R9W; about 300 ft. NW of Sta. 5	Greenstone	.96 fw[1/]
2	SE 1/4 sec. 14 T11N, R9W; about 0.4 mi. ESE Buckman Mine Hdg.	Cherty shale (JKs)	.91 f .95 f
3	NE 1/4 sec. 14 T11N, R9W; adjacent to Geyser Rd., 500 ft. ESE of Eagle Rock	Graywacke (JKms)	.93 f .94 w
4	NE 1/4 sec. 13, T11N, R9W; alteration zone about 500 ft. N of Power Plant A, on N side of main access rd.	Altered graywacke	.98
5	SE 1/4 sec. 11, T11N, R9W; Sta. 5	Graywacke (JKms)	.97 w
6	SE 1/4 sec. 14, T11N, R9W; 600 ft. E. of location 2	Greenstone	.96 f .96 w

---

1/ f = fresh

w = weathered

fw = partially weathered

(Table 1) show a spread in ε_{8-14} from 0.91 to 0.98, but more commonly from 0.94–0.97 for weathered surfaces. This variation in emissivity amounts to about 3°C for a 25°C surface temperature. However, soil development and generally rough surface textures probably tend to diminish the emissivity variable to a somewhat smaller value than suggested by the bedrock samples.

SUMMARY

The aerial infrared surveys indicate that the principal high temperature zones at The Geysers are in part limited (at the surface) on the southwest by structural lineaments; their northeast extent tends to be more diffuse.

An arcuate radiance pattern suggesting slightly elevated surface temperatures, extends beyond the northwest present limit of steam production at the Sulphur Banks. The arcuate zone seems to coincide with a temperature difference measured on the surface, and with a mapped fault, as well. There are other slightly elevated radiance patterns in Big Sulphur Creek valley but their significance is not known. The radiance in Big Sulphur Creek valley, except for the hydrothermal alteration zones, is not exceptional, that is, there is little evidence of a regional geothermal anomaly at the surface in The Geysers area.

ACKNOWLEDGEMENTS

The author is grateful to the Thermal Power Company for many courtesies extended during this study. Dr. James Koenig, Calif. Division of Mines, also provided much useful information, which is greatly appreciated.

Very competent assistance in the field was rendered by C. R. Fross who operated the infrared scanner, pilots Ray Rote, Howard Chapman and William Myers and technicians George Boynton, P. Philbin and R. M. Turner.

REFERENCES

Allen, E. T., and Day, A. L., 1927, Steam wells and other thermal activity at "The Geysers" California: Carnegie Inst., pub. no. 378, 106 p.

Bailey, E. H., 1946, Quicksilver deposits of the western Mayacamas District, Sonoma County, California: Calif. Journal Mines and Geol., v. 42, nO. 3, p. 199-230.

McNitt, J. R., 1963 (revised 1965), Exploration and development of geothermal power in California: Calif. Div. Mines and Geol., Special Report 75, 45 p.

Moxham, R. M., Greene, G. W., Friedman, J. D., and Gawarecki, S. J., 1968, Infrared imagery and radiometry summary report, Dec. 1967: U. S. Geol. Survey Interagency Report NASA-105, open-file report, 29 p.

Otte, C., and Dondanville, R. F., 1968, Geothermal developments in The Geysers area, California (abstract): Amer. Assn. Petrol. Geol., Symposium on geothermal resources, March 29, Bakersfield, Calif.

Turner, R. M., and Boynton, G. R., 1968, Film density analyzers for infrared investigations: U. S. Geol. Survey Interagency Report NASA-94, open-file report.

Figure 1. Location map.

FIG. 1

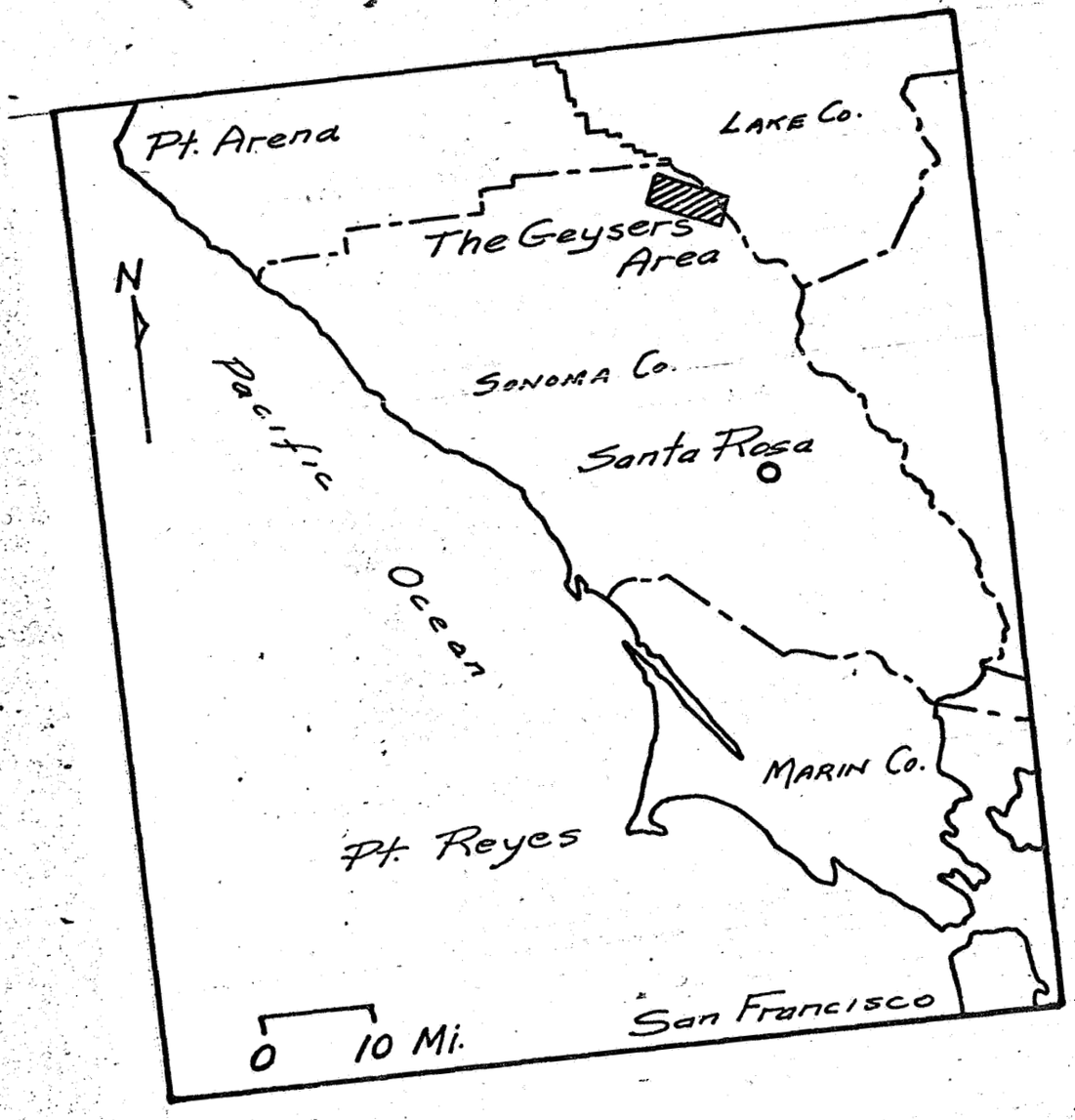
Pt. Arena
LAKE CO.
The Geysers Area
N
SONOMA CO.
Pacific Ocean
Santa Rosa
MARIN CO.
Pt. Reyes
0 10 Mi.
San Francisco

Figure 2. Topographic map of the report area. The approximate boundaries of some of the other illustrations in this report are shown by the rectangles. Area of hydrothermal alteration, taken from Bailey (1946) are indicated by gray patches. Approximate limit of the producing wells of the streamfield in December, 1967 is indicated by the dashed line. Other wells drilled for stream are indicated by triangles: A=Signal Oil and Gas Wild Mtn. no. 2; B=Powerhouse no. 2; C=Signal Oil and Gas Wild Horse no. 1; D=Signal Oil and Gas Cobb Mtn. no. 1; E=Geothermal Resources Inc., no. 1; F=Geothermal Resources Inc., no. 2; G=Union Oil Ottobani no. 1; H=Geothermal Development Company, 65-28; J=Little Geysers no. 2; K=Little Geysers no. 1; L=D and V 73-33 (started 9/68) Letter; M=Little Geysers; N=Sulphur Banks.

FIGURE 2

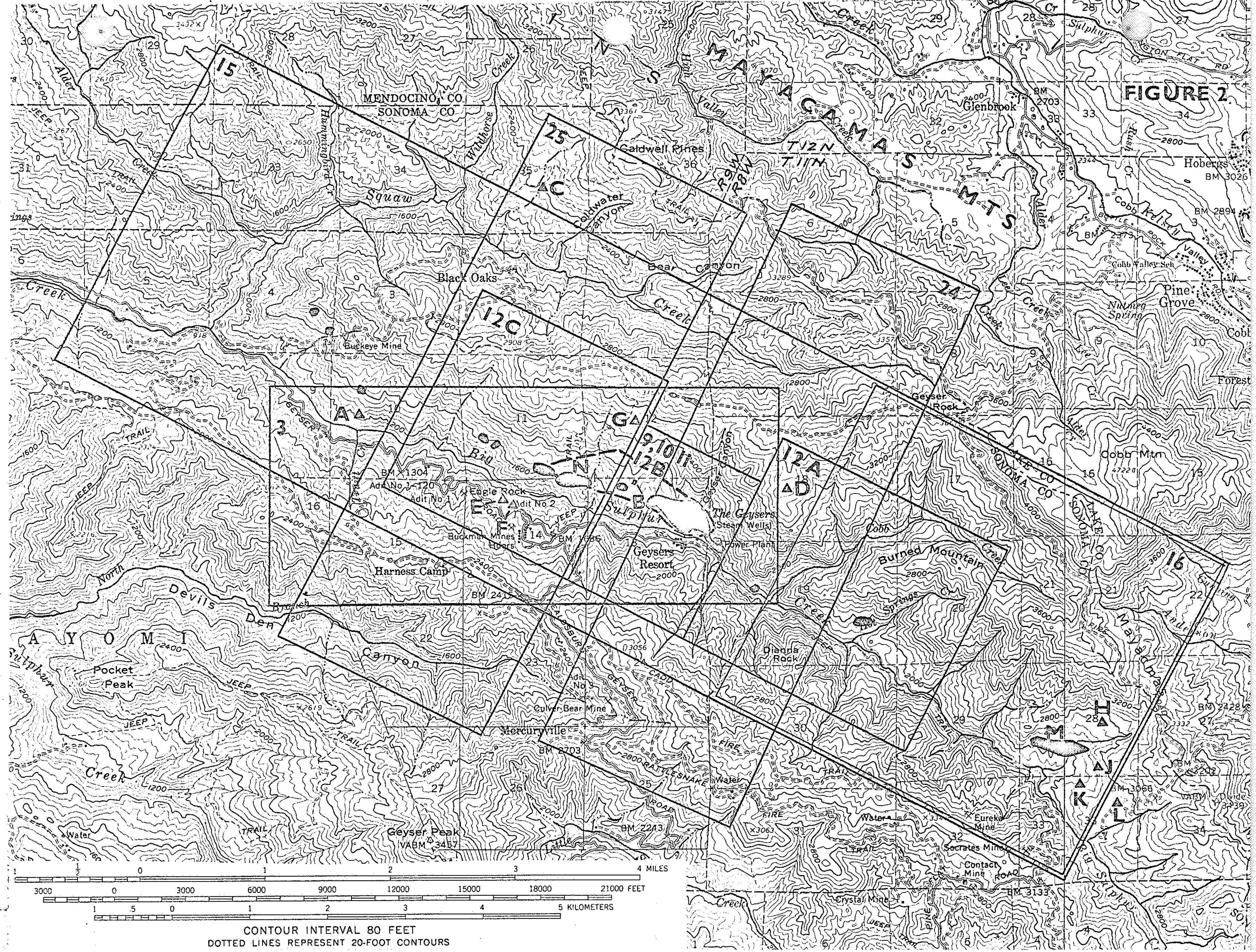

MAYACAMAS MTS
MENDOCINO CO
SONOMA CO
LAKE CO
SONOMA CO
T12N
T11N
R9W
R8W
Caldwell Pines
Glenbrook
Hobergs
Pine Grove
Cobb Mtn
Black Oaks
Bear Canyon
Geyser Rock
Buckeye Mine
Eagle Rock
Adit No 1
Adit No 2
Buckman Mines
The Geysers (Steam Wells)
Power Plant
Geysers Resort
Harness Camp
Burned Mountain
Dianna Rock
Culver-Bear Mine
Mercuryville
Devils Den Canyon
Pocket Peak
Geyser Peak
VABM 3457
Eureka Mine
Socrates Mine
Contact Mine
Crystal Mine
Squaw
Coldwater Canyon
Big Sulphur
15
25
24
12C
12A
9,10,11
12B
3
16
A
B
C
D
E
F
G
H
J
K
L
M
N
1 ½ 0 1 2 3 4 MILES
3000 0 3000 6000 9000 12000 15000 18000 21000 FEET
1 .5 0 1 2 3 4 5 KILOMETERS
CONTOUR INTERVAL 80 FEET
DOTTED LINES REPRESENT 20-FOOT CONTOURS

Figure 3. Geologic map of The Geysers area from McNitt, 1963. A=power plant no. 1; B=power plant no. 2; C=Eagle Rock; D=Geyser Road; E=Healdsburg-Geyser Road; geothermal steam wells are indicated by circles.

Geologic formations are indicated by the following symbols: Franciscan formation (Jurassic-Cretaceous) from base upward; solid cross hatch=graywacke and shale (JKs); gray=greenstone (gs); broken cross hatch=serpentine (sp); white=micaceous graywacke and shale (JKms); barbed boundaries enclose landslides of Pliocene age.

FIG 3

Geology from McNitt, 1963

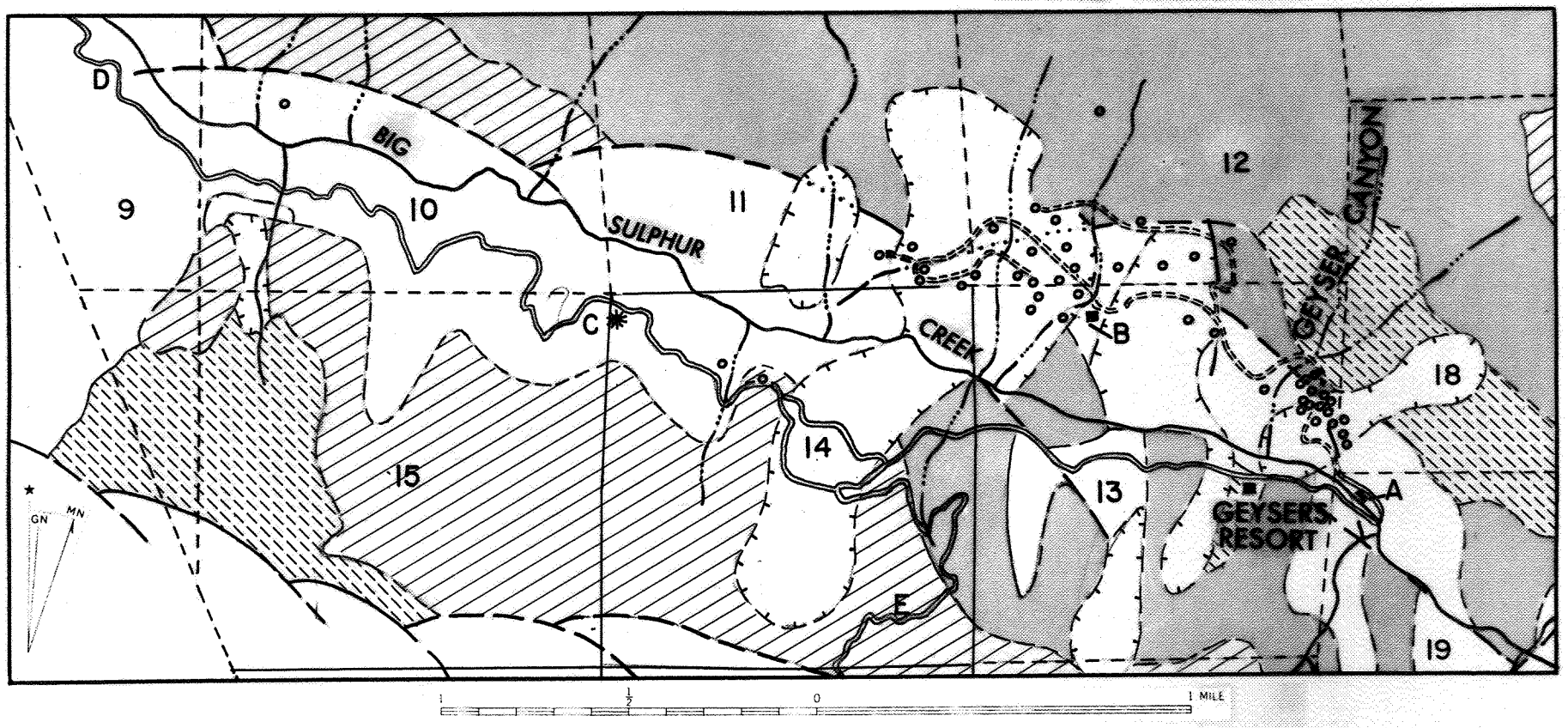

Figure 4. Relation between insolation and surface temperature. Insolation was measured with an Eppley 180° pyranometer (X). Between the first light of dawn (A) and local sunrise (B), sky radiation was less than the detection limit of the pyranometer. First light was detected with an uncalibrated cadmium sulfide cell (+) which recorded a full scale deflection from 06.00 to 06:30, and is shown here on an arbitrary scale. Surface temperature was measured with a thermistor buried 3 mm beneath the ground surface. (o)

FIGURE 4

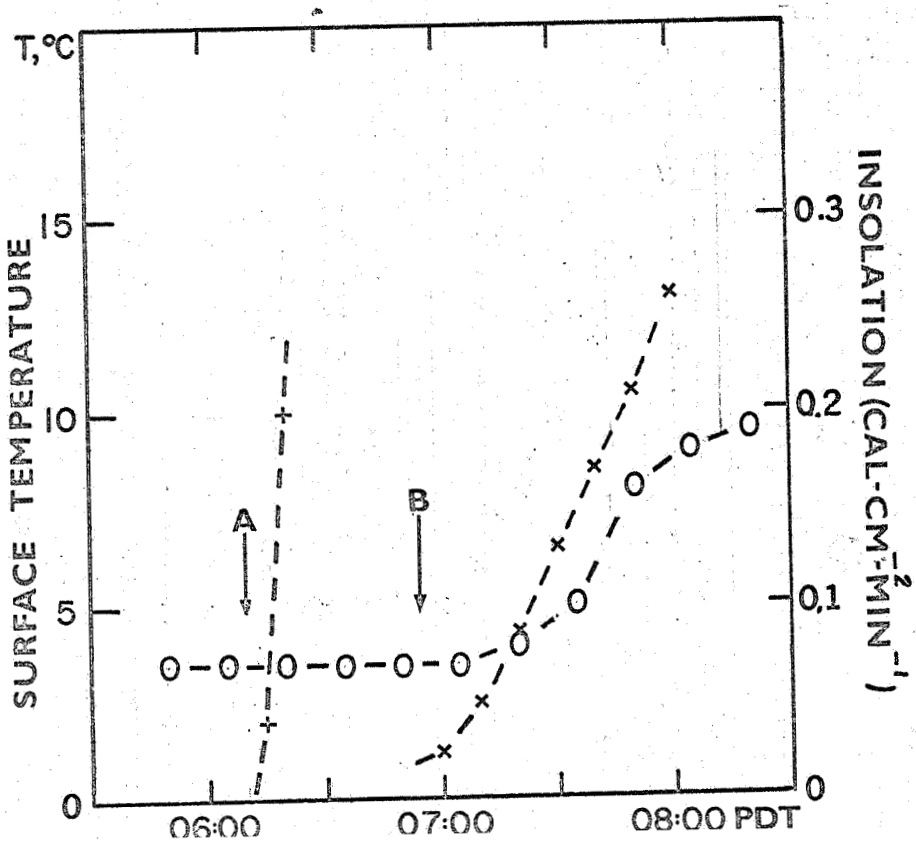
T,°C
SURFACE TEMPERATURE
INSOLATION (CAL-CM⁻²MIN⁻¹)
0
5
10
15
0
0.1
0.2
0.3
A
B
06:00
07:00
08:00 PDT

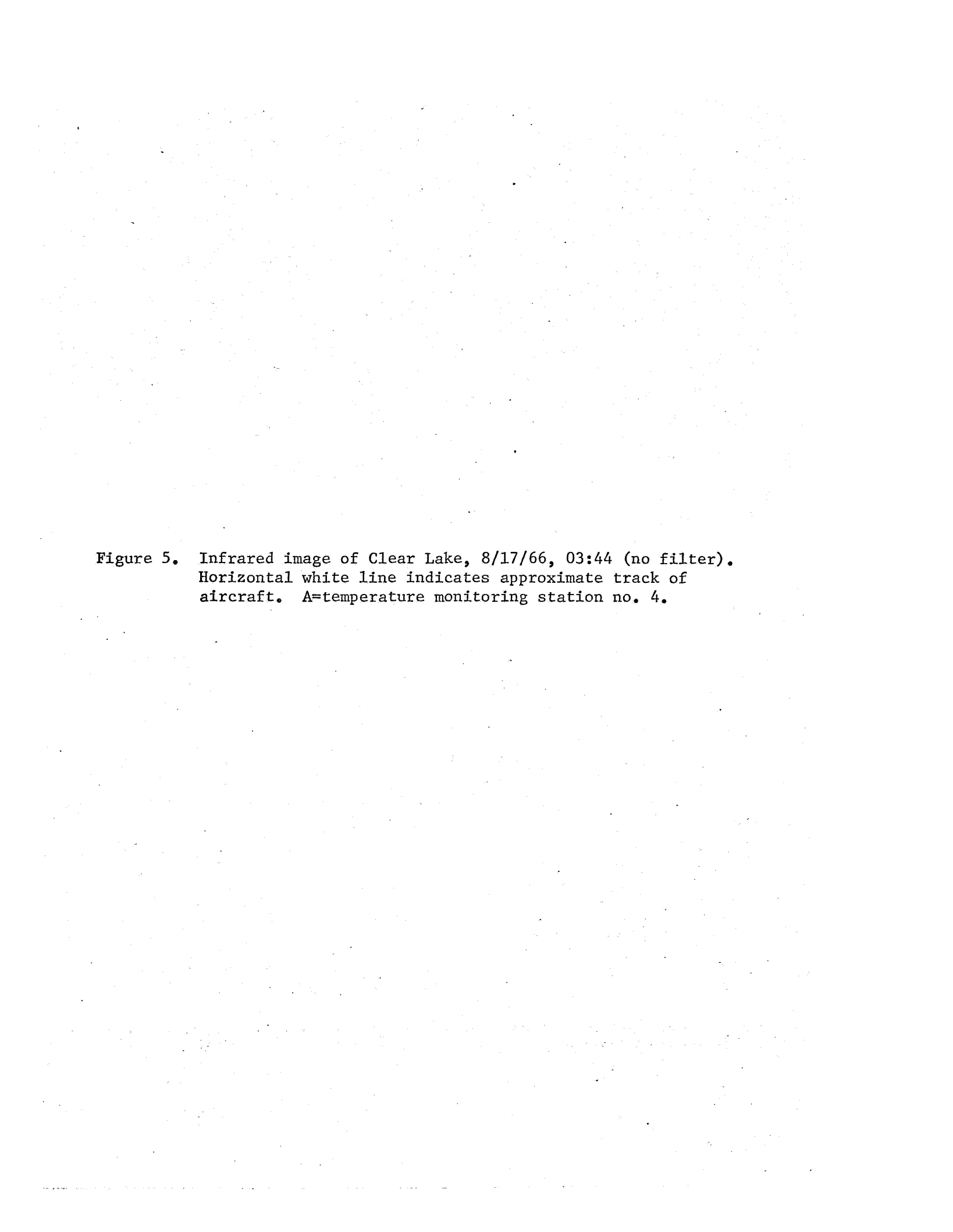

Figure 5. Infrared image of Clear Lake, 8/17/66, 03:44 (no filter). Horizontal white line indicates approximate track of aircraft. A=temperature monitoring station no. 4.

FIG. 5

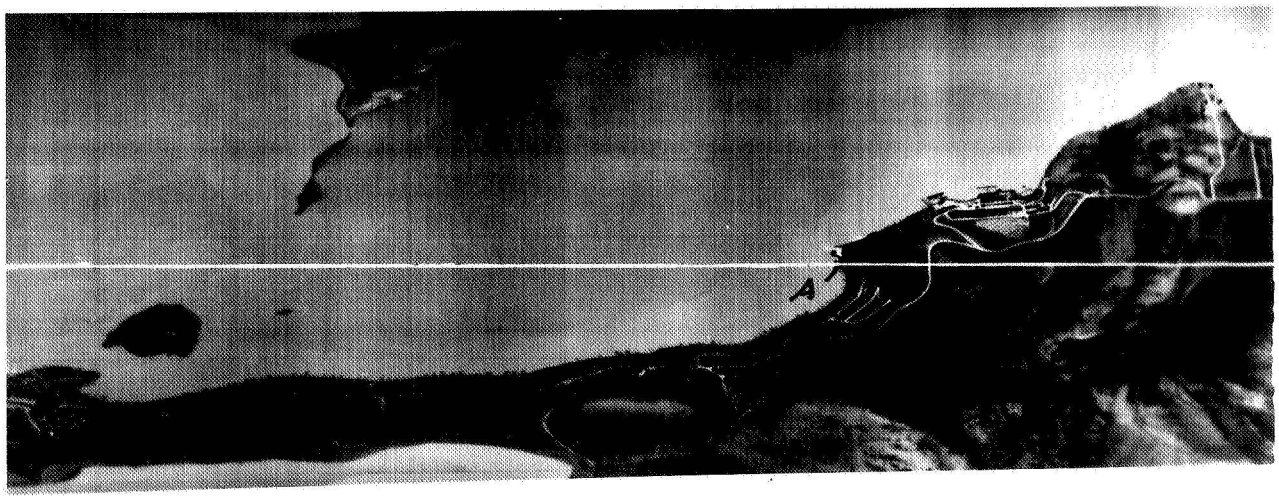

Figure 6. MDT density profiles of the Clear Lake image (figure 5) along the flight path. Temperatures of the land and water are those measured at station 4.

FIG. 6A

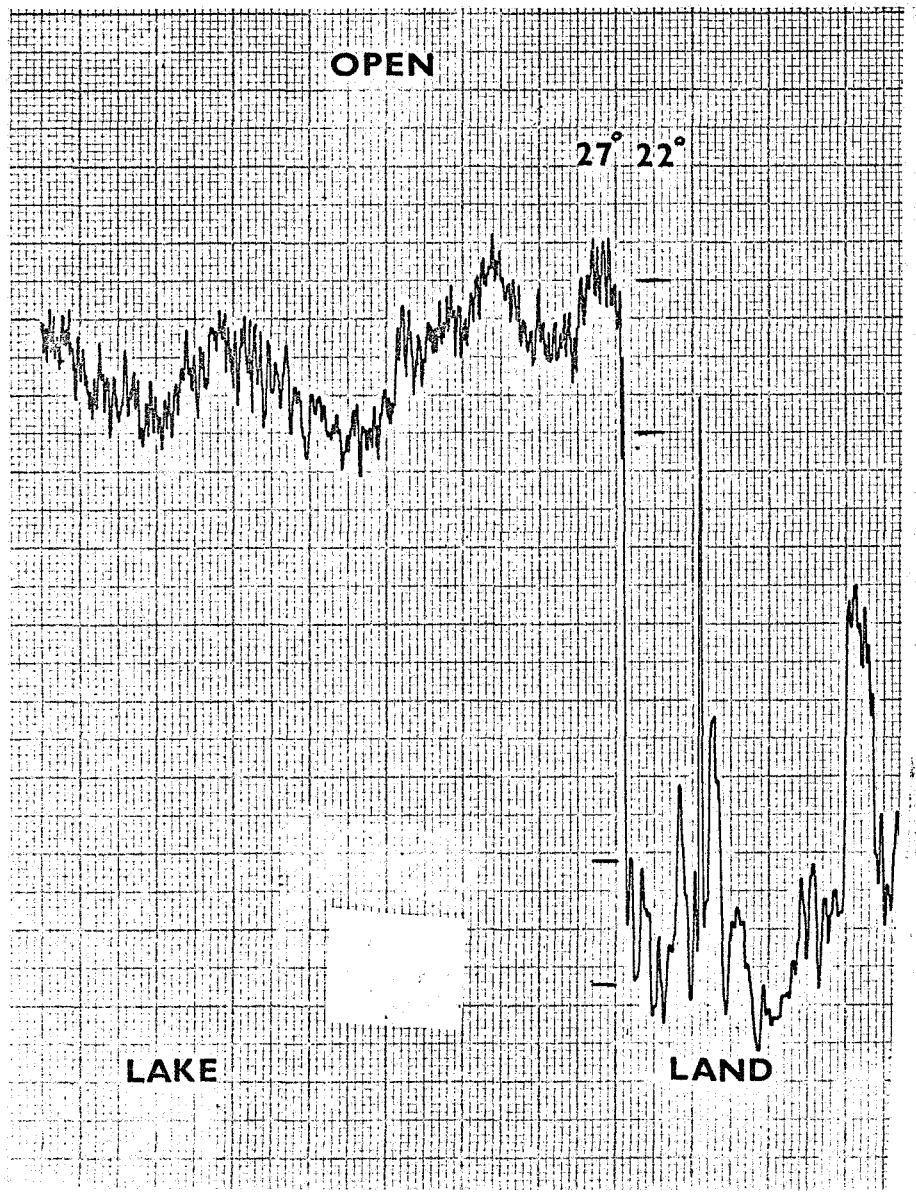
OPEN
27° 22°
LAKE
LAND

FIG. 6B

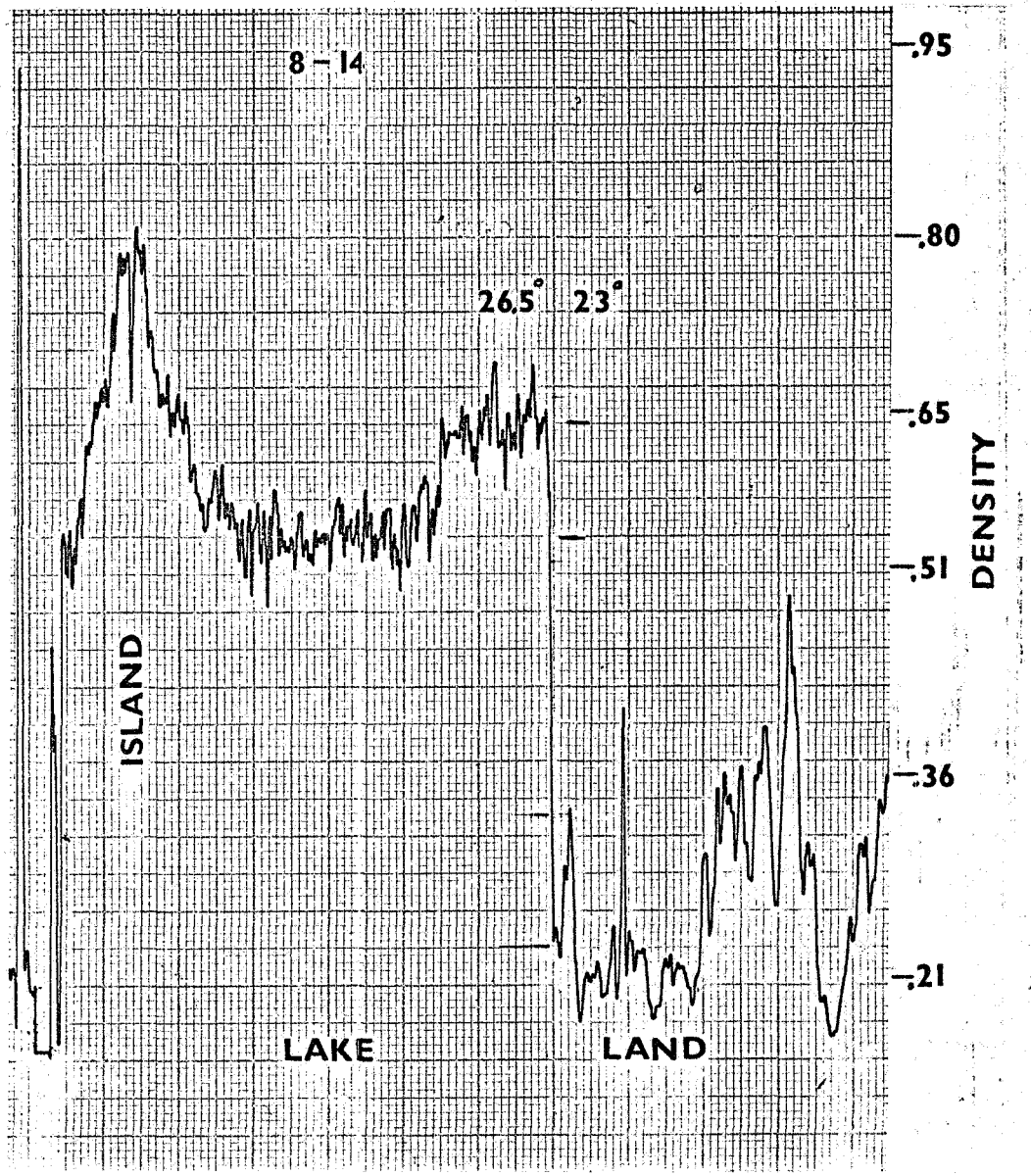
8 – 14
26.5° 23°
ISLAND
LAKE
LAND
.95
.80
.65
.51
.36
.21
DENSITY

FIG. 6C

FIG. 6D

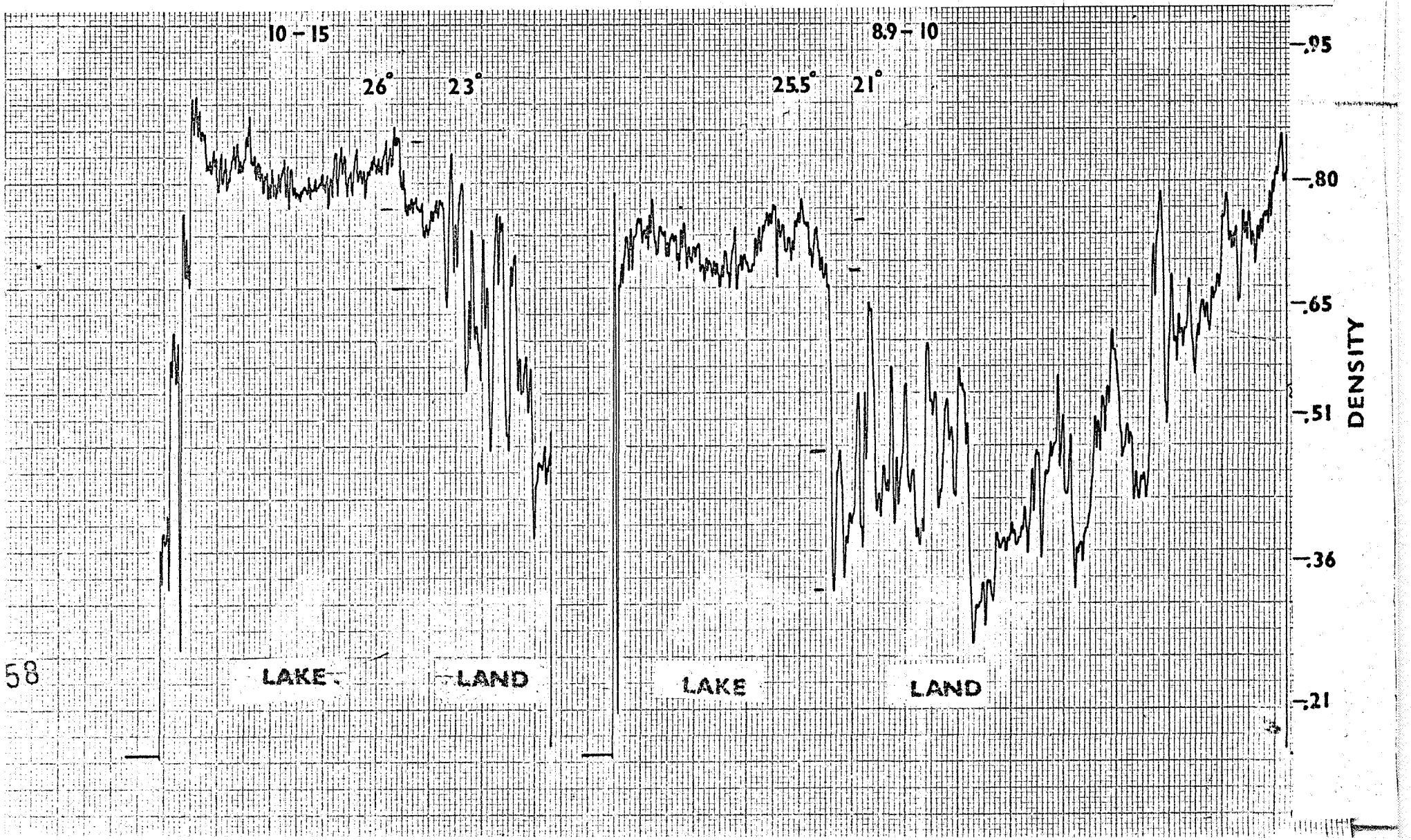
10 – 15
26°
23°
LAKE
LAND
8.9 – 10
25.5°
21°
LAKE
LAND
.95
.80
.65
.51
.36
.21
DENSITY

Figure 7. MDT density profile at Clear Lake (figure 5) across the flight path. Arrows indicate the lateral limits of the terrain scan.

FIG. 7C

FIG. 7B

FIG. 7A

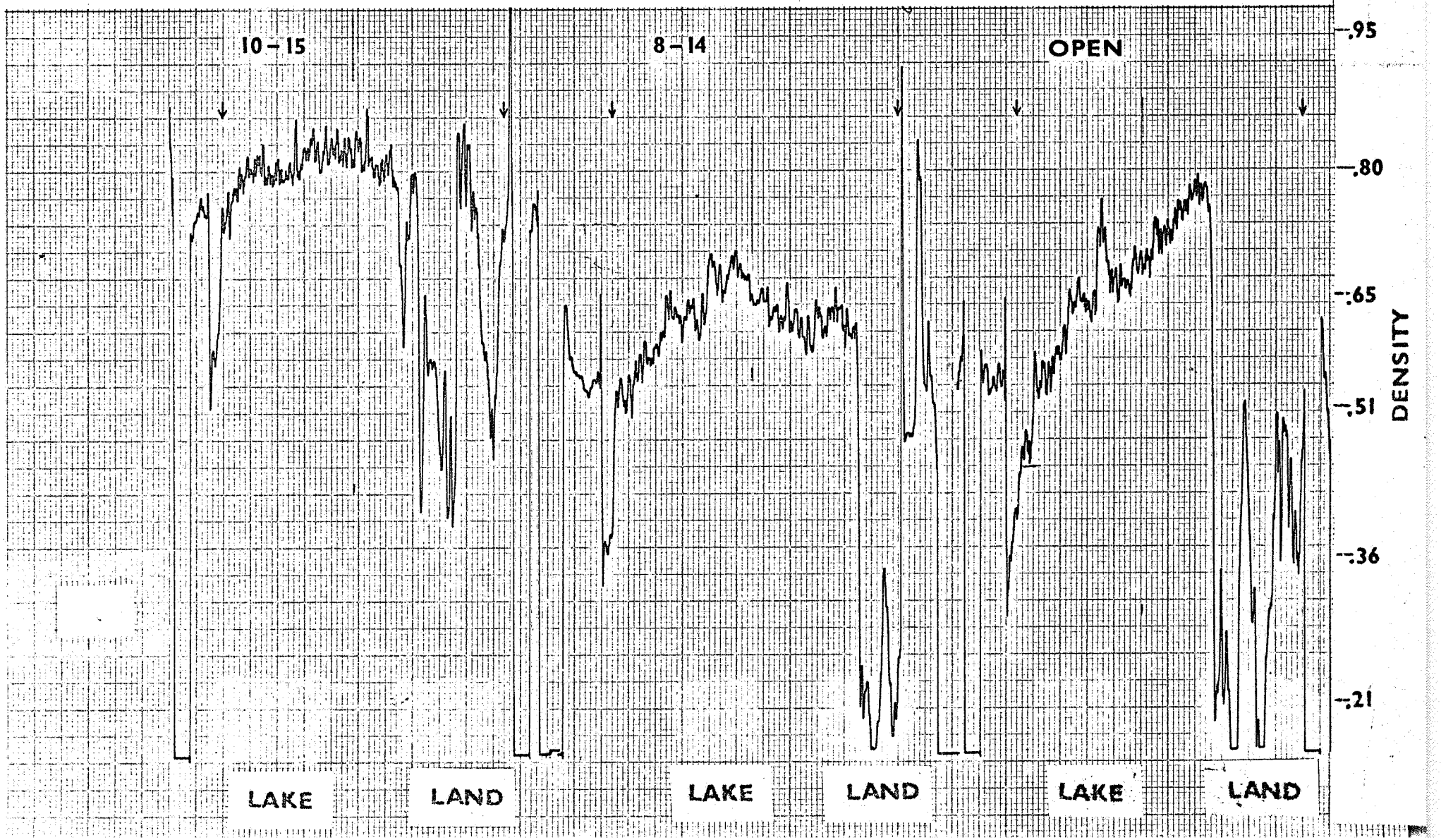

FIG. 7D

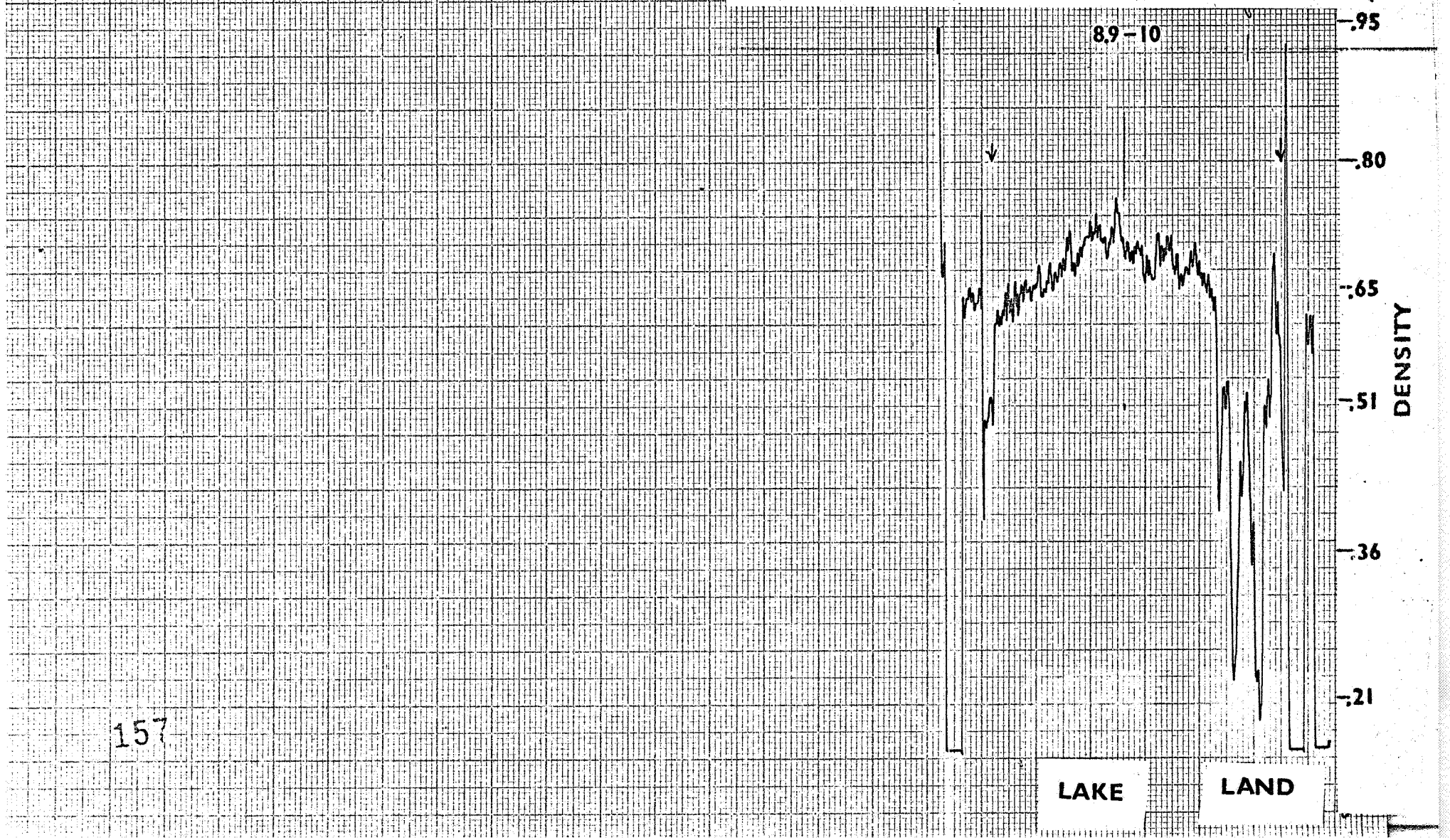

Figure 8. Image density vs terrain temperature along flight path (right) and across flight path (left). Solid lines indicate limit of error for 8-14μm pass band.

FIG. 8

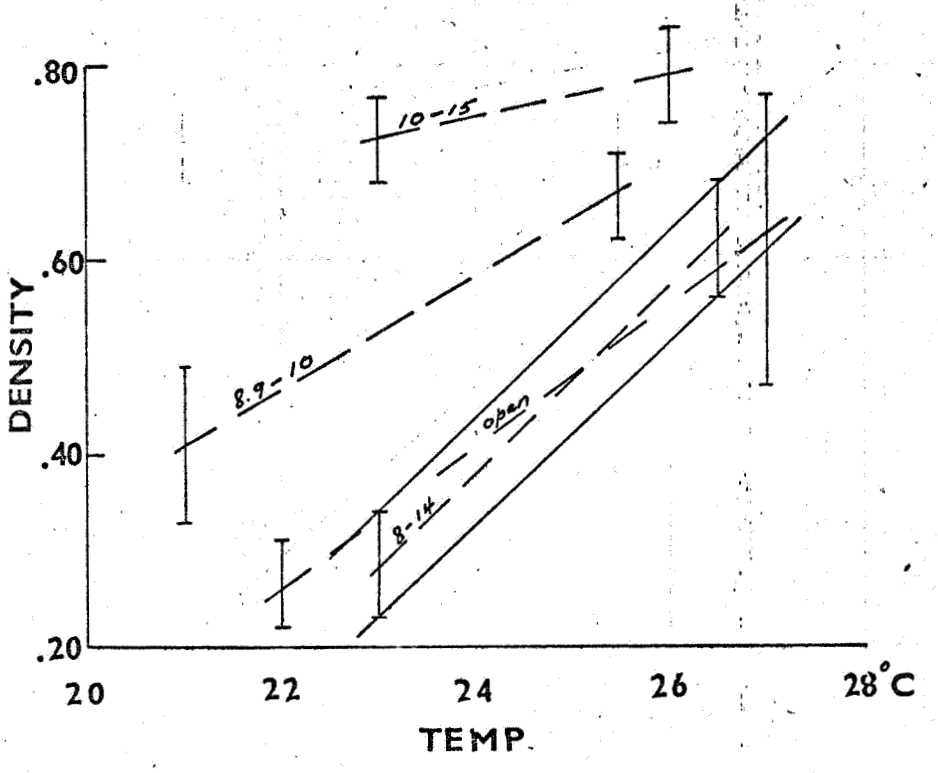
.80
.60
.40
.20
DENSITY
10-15
8.9-10
open
8-14
20
22
24
26
28°C
TEMP.

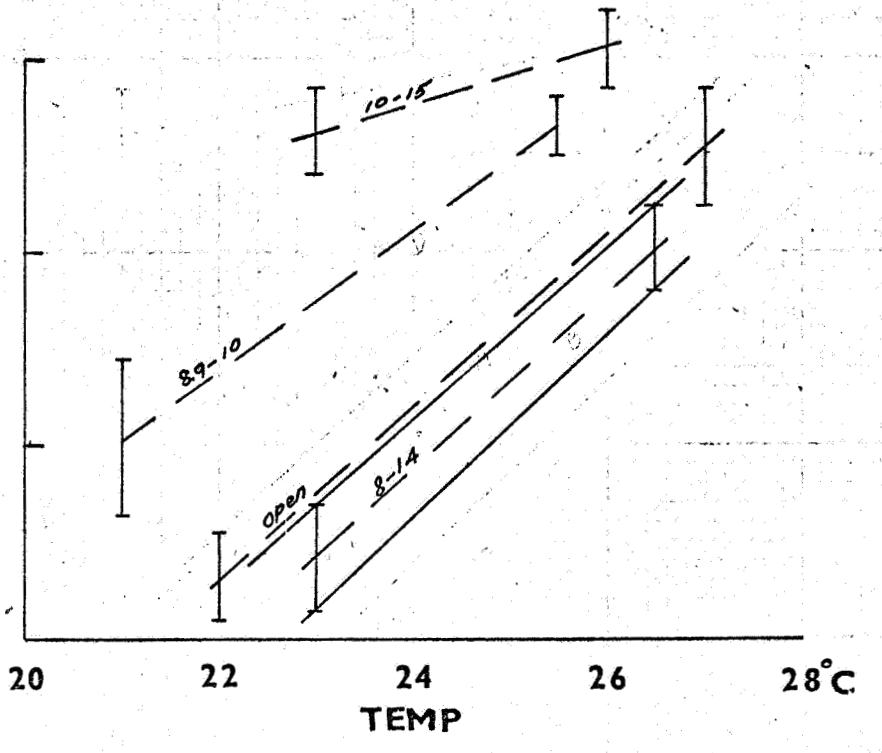
10-15
8.9-10
open
8-14
20
22
24
26
28°C
TEMP

Figure 9. 1955 aerial photo of the steam-production area at The Geysers. White patches are zones of hydrothermal alteration. Figures 10, 11, and 12B cover approximately the same area.

FIG. 9

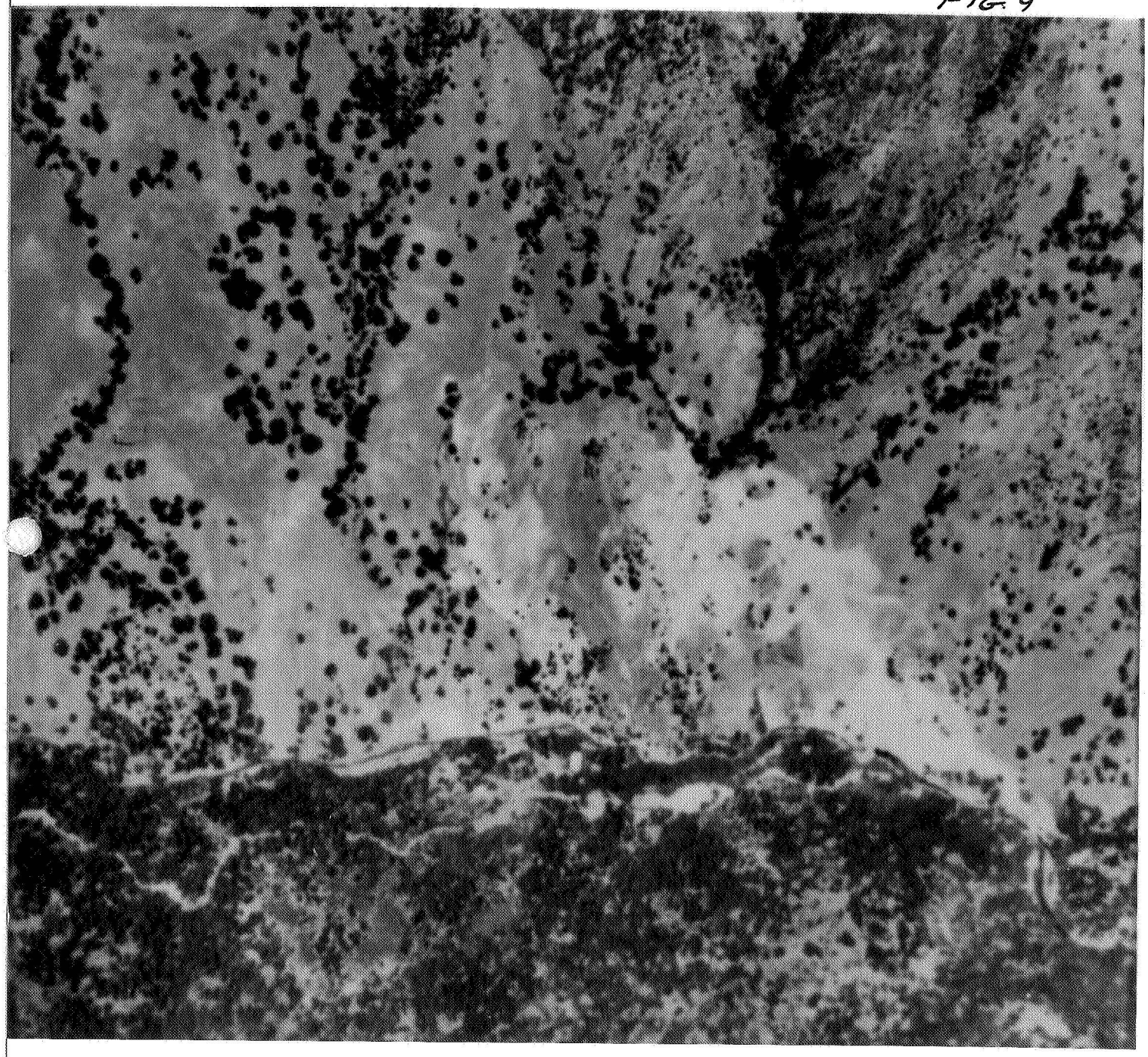

Figure 10. 1966 aerial photo of the steam-production area at The Geysers. Power plant no. 1 is on the lower right; power plant no. 2 is at the left center.

FIG. 10

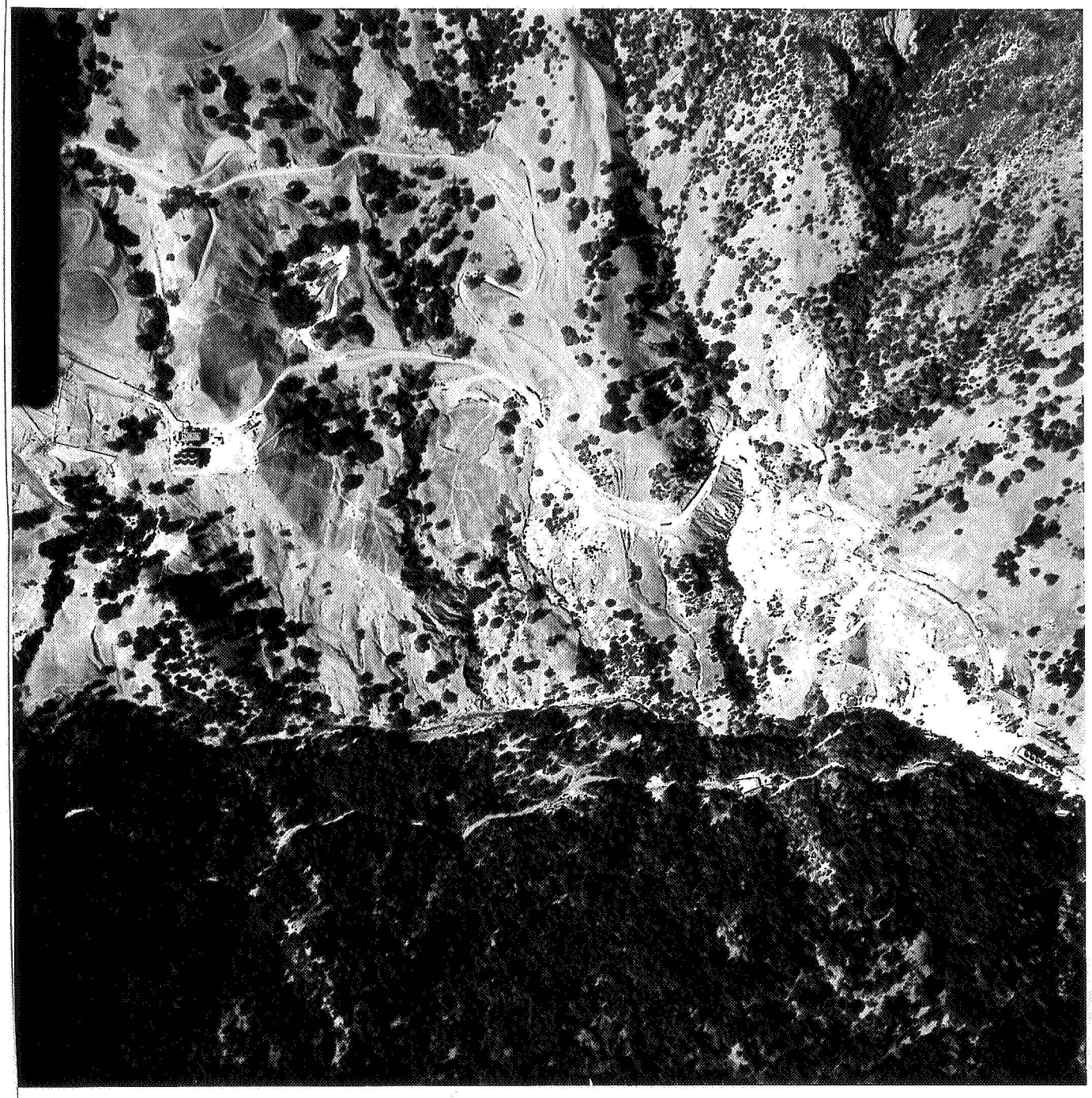

Figure 11. Daytime IR image of the steam production area at The Geysers (15:34, August 16, 1966). Arrow indicates ring-shaped thermal anomaly surrounding blown-out steam well.

FIG. 11

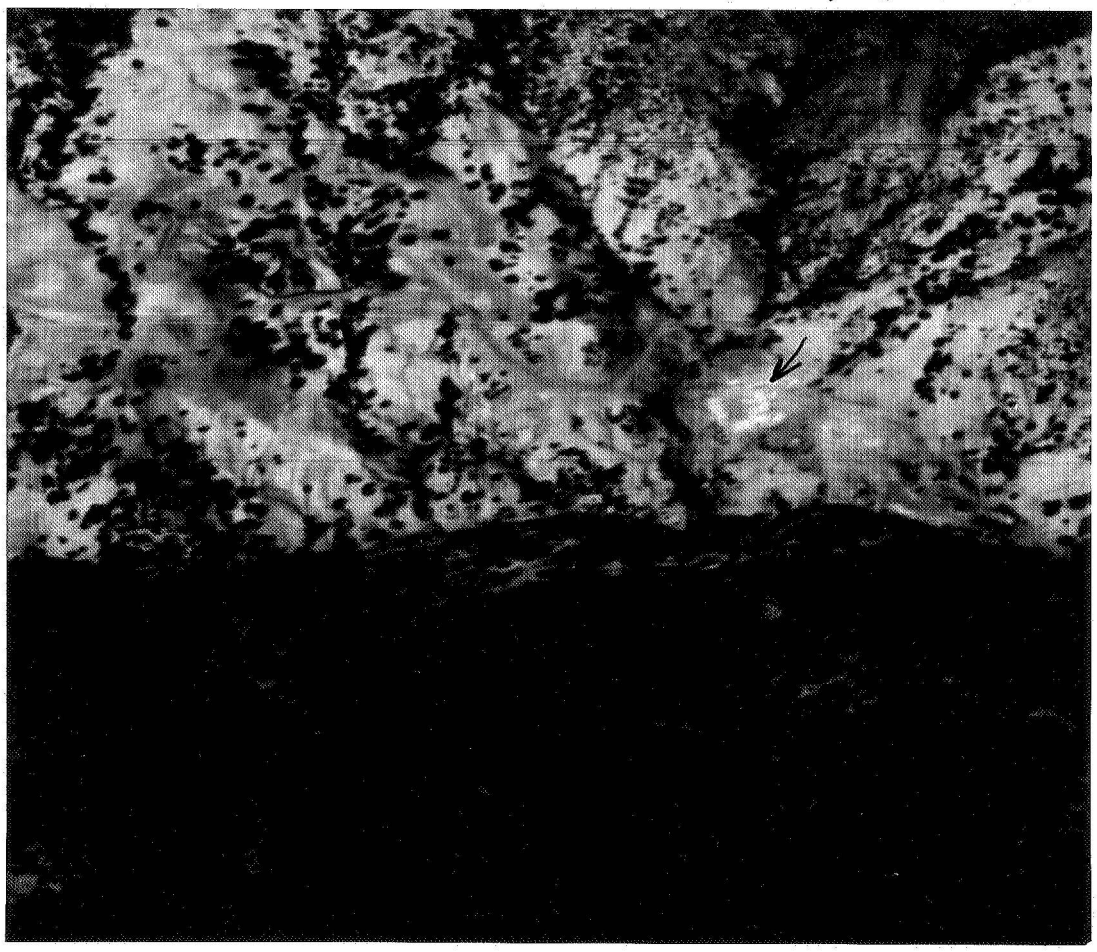

Figure 12A. Predawn IR image of Big Sulphur Creek valley. In three overlapping views: 12A, area southeast of The Geysers; 12B, The Geysers; 12C, area northwest of The Geysers.

12A: A=Hot Springs (?); B=Hot Springs Creek; C=Cobb Creek; D=power house no. 1.

FIG. 12 A

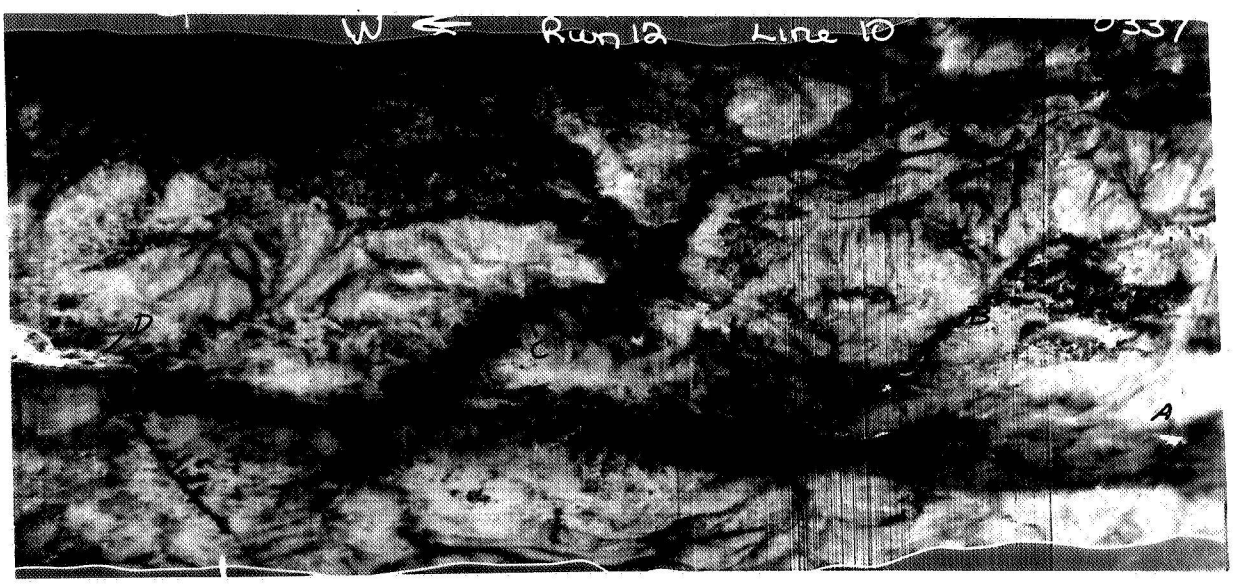

Figure 12B. A=Big Sulphur Creek; B=Geyser Road; C=The Geysers resort; D=power plant no. 1; E=power plant no. 2. Power plant no. 1, in operation shows warm; power plant no. 2, under construction shows cold.

FIG. 12 B

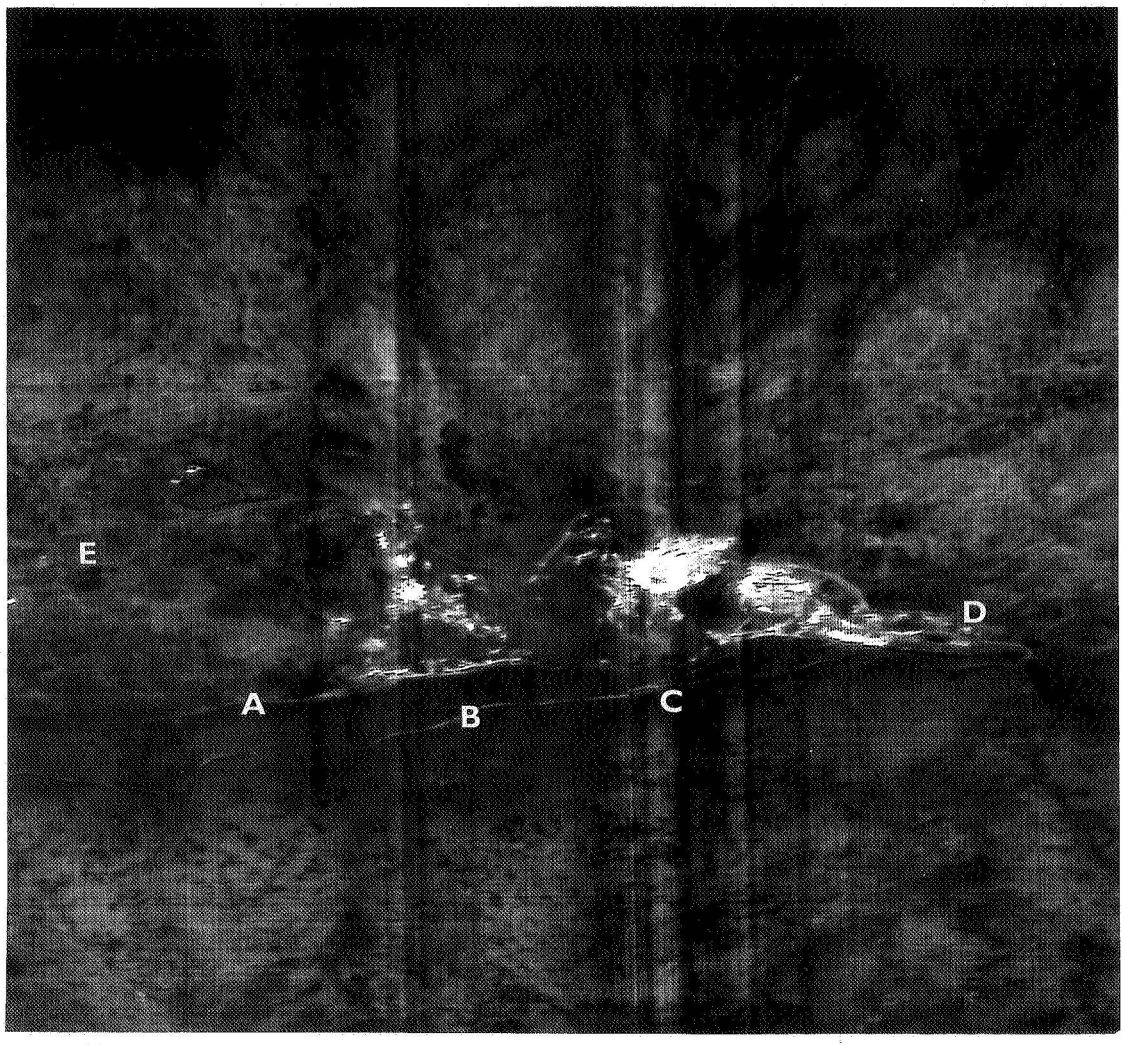

Figure 12C. A=temperature monitoring station no. 1; B=station no. 2; C=station no. 3; D=Geyser Road; E=Healdsburg-Geyser Road; F=Big Sulphur Creek; G=jeep trail; H=Eagle Rock.

FIG 12C

Figure 13. 1966 aerial photo of the Sulphur Banks. Power plant no. 2 is in the lower center. Temperature monitoring stations are indicated by the numbers 1, 2, and 5.

FIG. 13

Figure 14. Surface temperature observations at the Sulphur Banks. Images shown in figures 11 and 12 were made during the infrared surveys on 8/16 and 8/17 respectively (arrows).

Station locations are shown on figure 12C. Brackets show temperature spread among the three thermistors at each station at time indicated.

FIG. 14

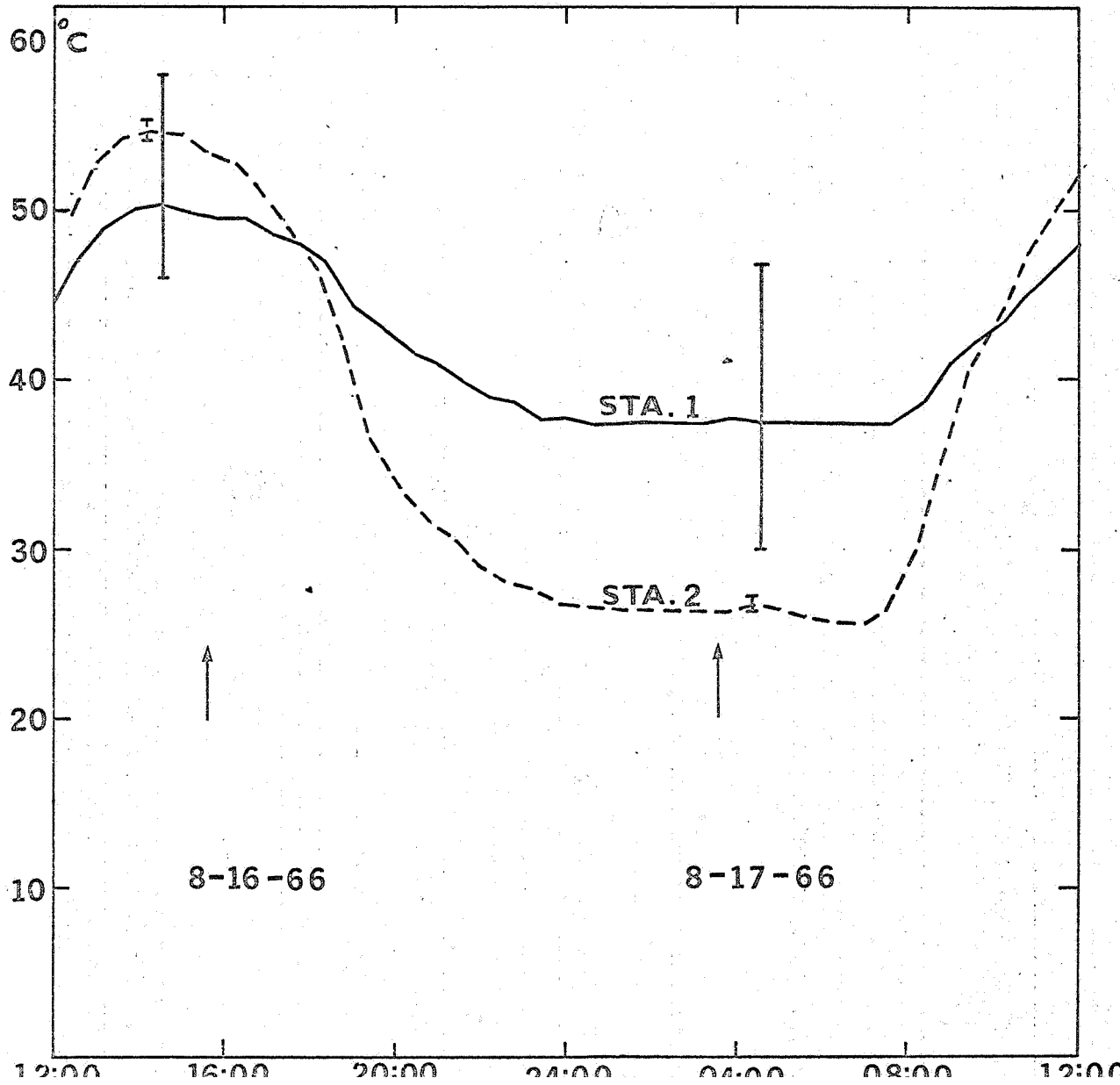
60 °C
50
40
30
20
10
STA. 1
STA. 2
8-16-66
8-17-66
12:00
16:00
20:00
24:00
04:00
08:00
12:00

Figure 15. Infrared image of Big Sulphur Creek valley (8/17/66, 04:00, no filter). A=Big Sulphur Creek; B=Squaw Creek; C=The Sulphur Banks; D=The Geysers; E=Little Geysers. A row of white dots on the lower right of the image is caused by static electricity discharge.

FIG. 15

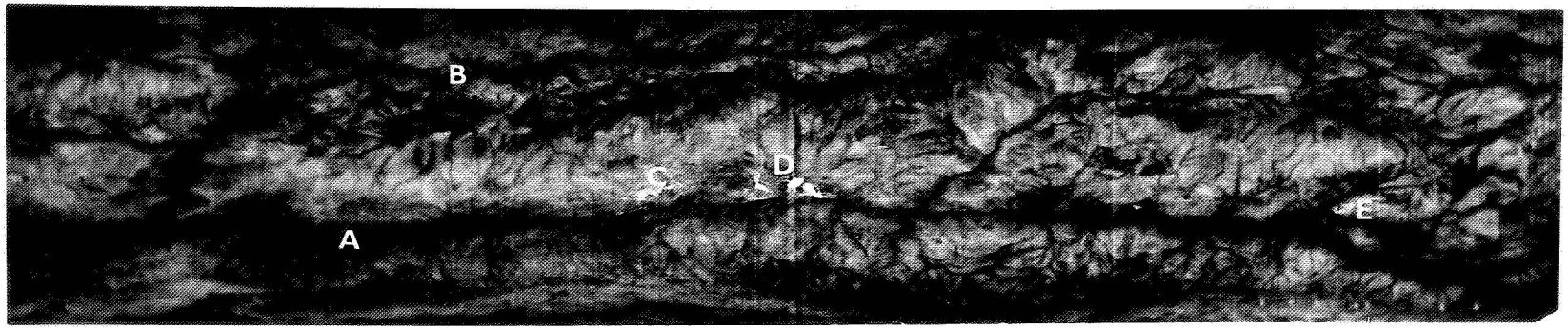

Figure 16. Infrared image of the Little Geysers area (04:00, 8/17, no filter). A=Big Sulphur Creek, B=Cobb Creek; C=Hot Springs Creek; D=Little Geysers. Figure 16 is an enlargement of the SE part of figure 15.

FIG. 16

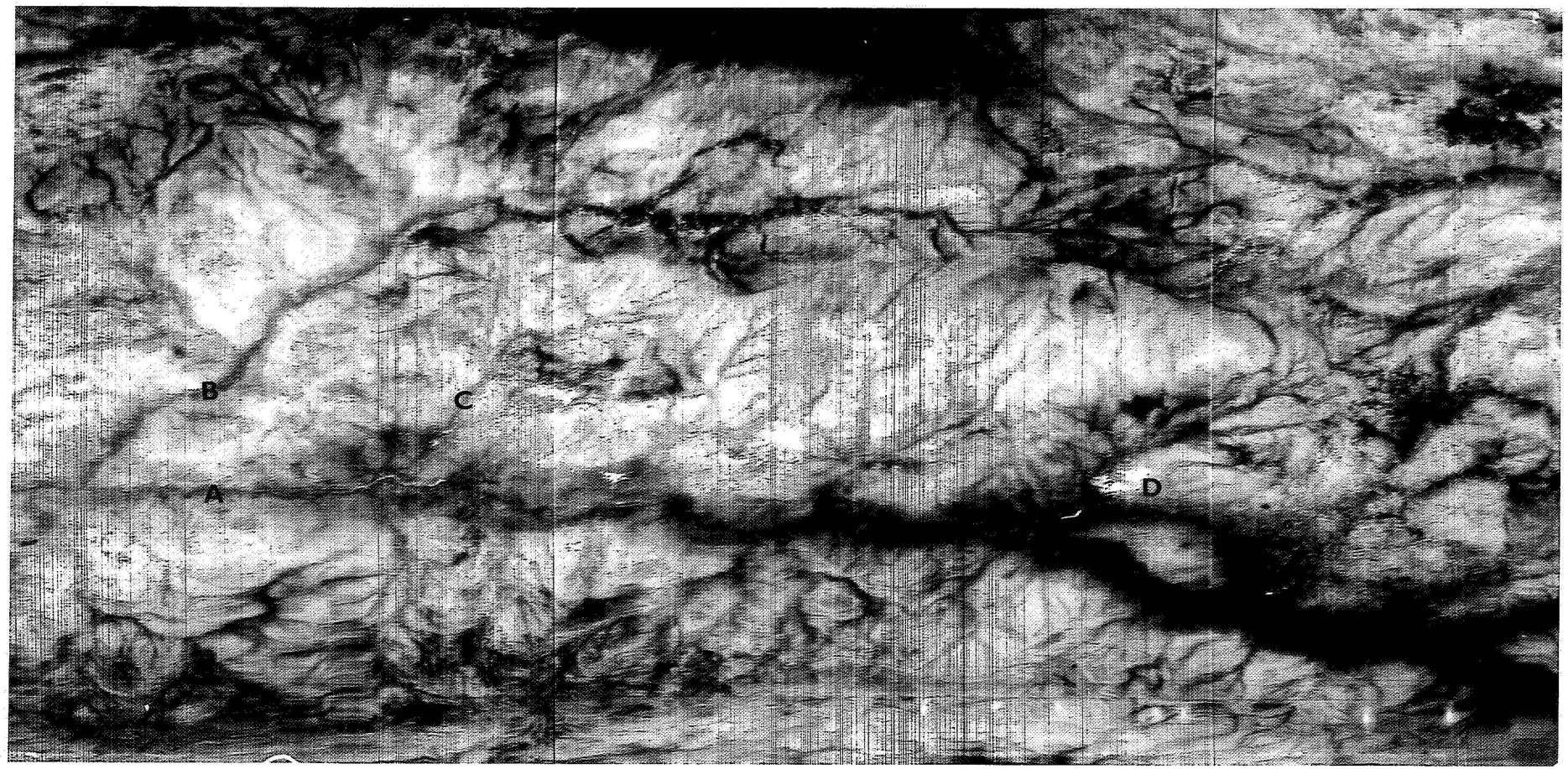

Figure 17. Steaming fracture along Big Sulphur Creek. Power plant no. 2 is in the background on the upper left.

FIG. 17

Figure 18. Tech/Ops film density map of part of fig. 12. Top view is the density slice showing only maximum densities. Lower densities are added by increments toward the bottom.

FIG. 18

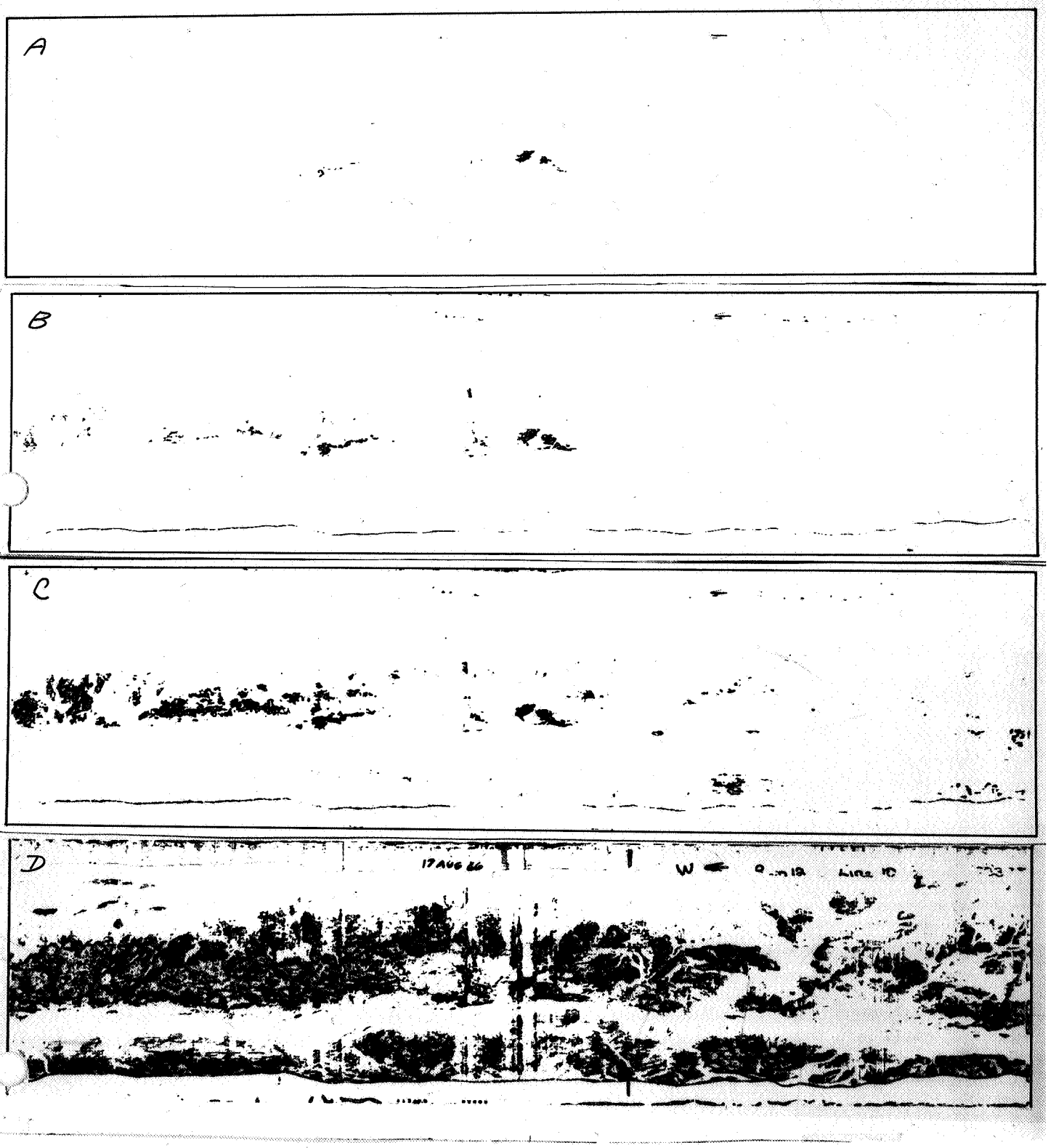

Figure 19. Enlargement of part of figure 18B with landmarks superimposed. Dashed lines are jeep trails. A=Geyser Road; B=Healdsburg-Geyser Road; C=power plant no. 2; E=Eagle Rock. Segments of stream valleys have been shown where they can be identified.

FIG. 19

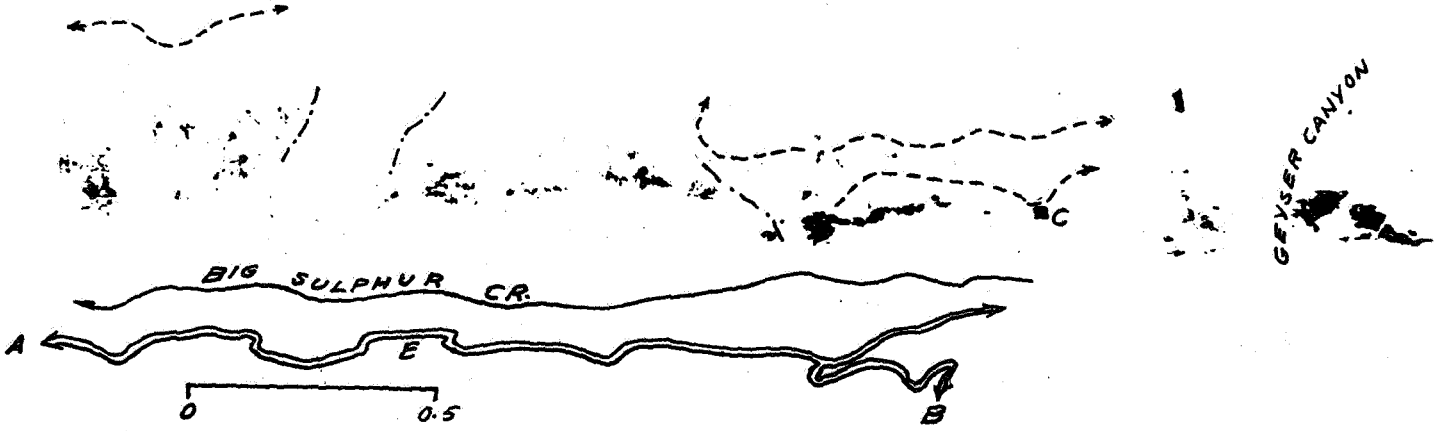

Figure 20. IDT-MDT isodensity map of part of figure 12. A=Geyser Road; B=Geyser-Healdsburg Road; C=power plant no. 2; E=Eagle Rock. Maximum density shown in black; second highest density shown by dashed contour. Segments of private roads and jeep trails are shown only where they can be identified on the image.

FIG. 20

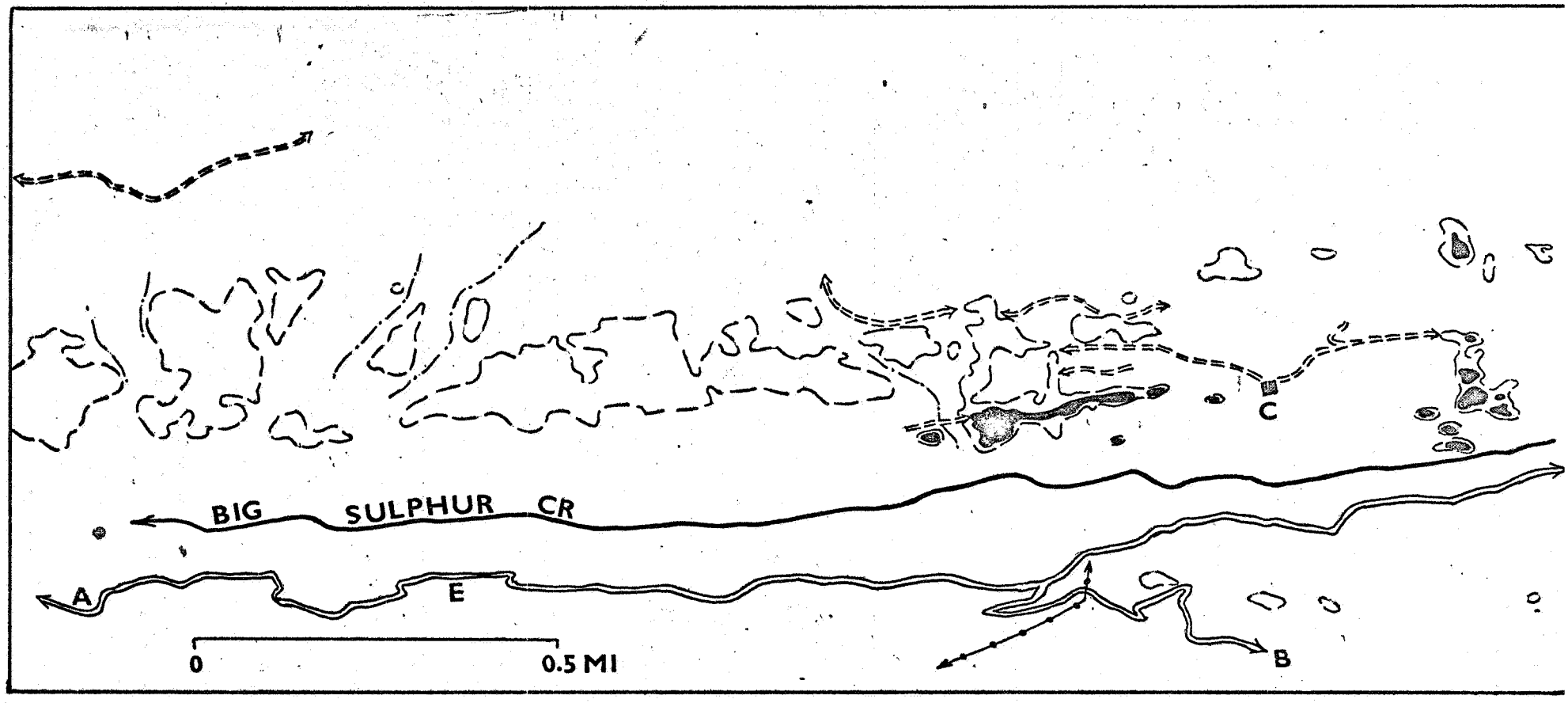

Figure 21. IDT-MDT isodensity map of figure 15. A=Geyser Canyon; B=power plant no. 2; C=power plant no. 1; D=The Geysers resort; E=Hot Springs Creek; F=Eagle Rock. Maximum density shown in black; second and third highest densities indicated by solid and dashed contours respectively.

FIG. 21

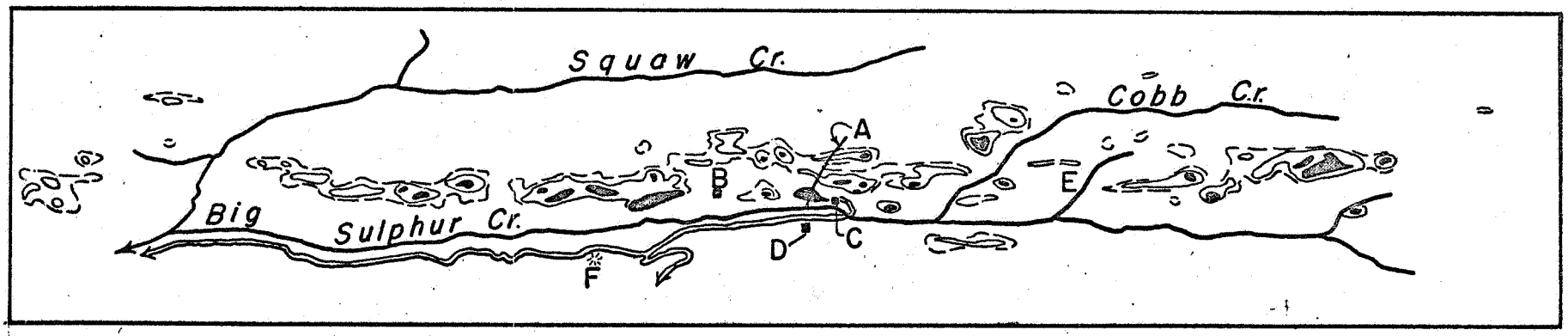

Figure 22. Surface temperatures at station 5 across the fault (?) west of the Sulphur Banks. Each curve represents the temperature recorded by one thermistor. The thermistors were placed in a NE-SW line spaced at fifty foot intervals. The two lower curves (solid line and long dashes) represent the two thermistors on the SW.

FIG. 22

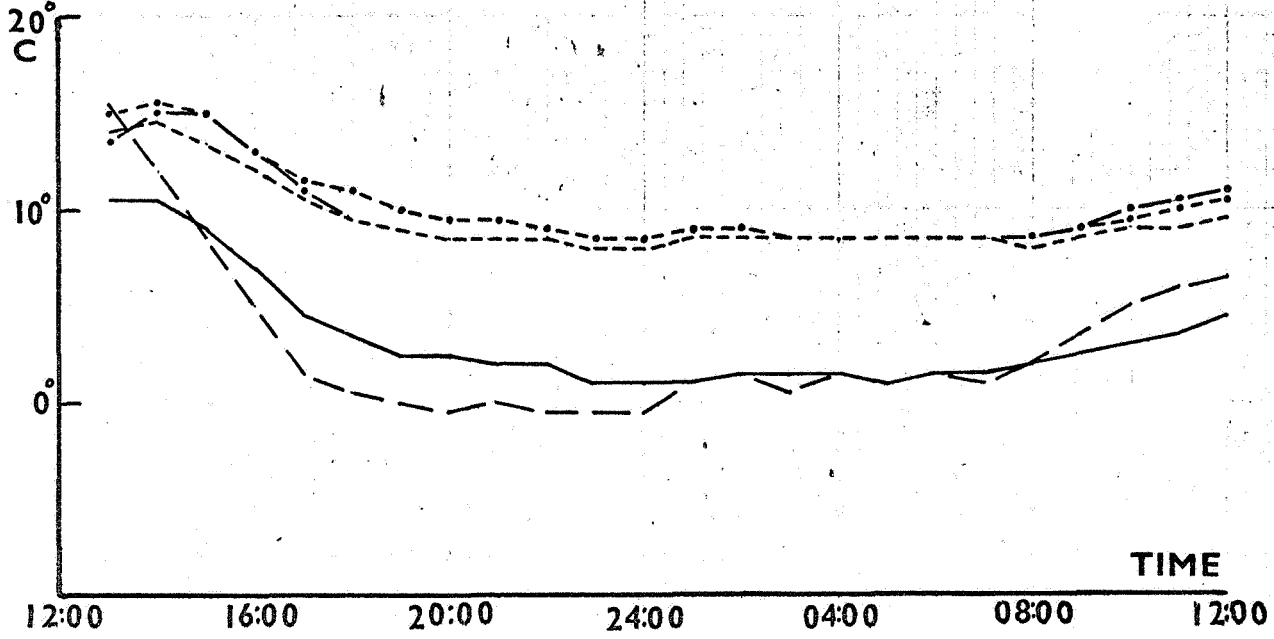

Figure 23. IR images of The Geysers steam field showing effects of band pass filter. Top, 8.9-10 micrometers, 03:50, 8/18/66. Bottom, no filter, 04:00, 8/17/66.

FIG. 23

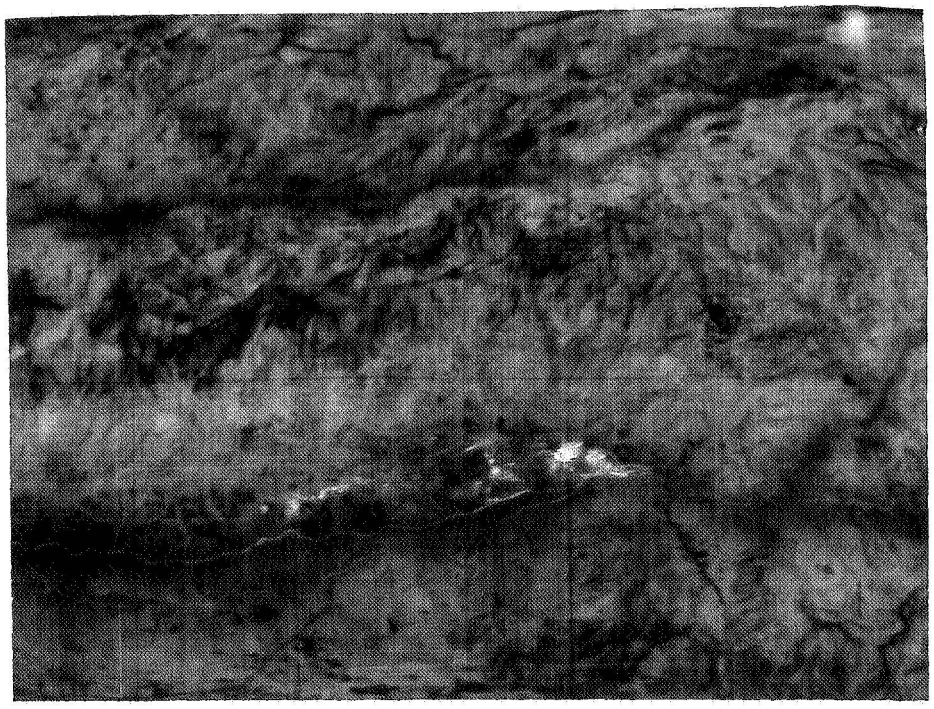

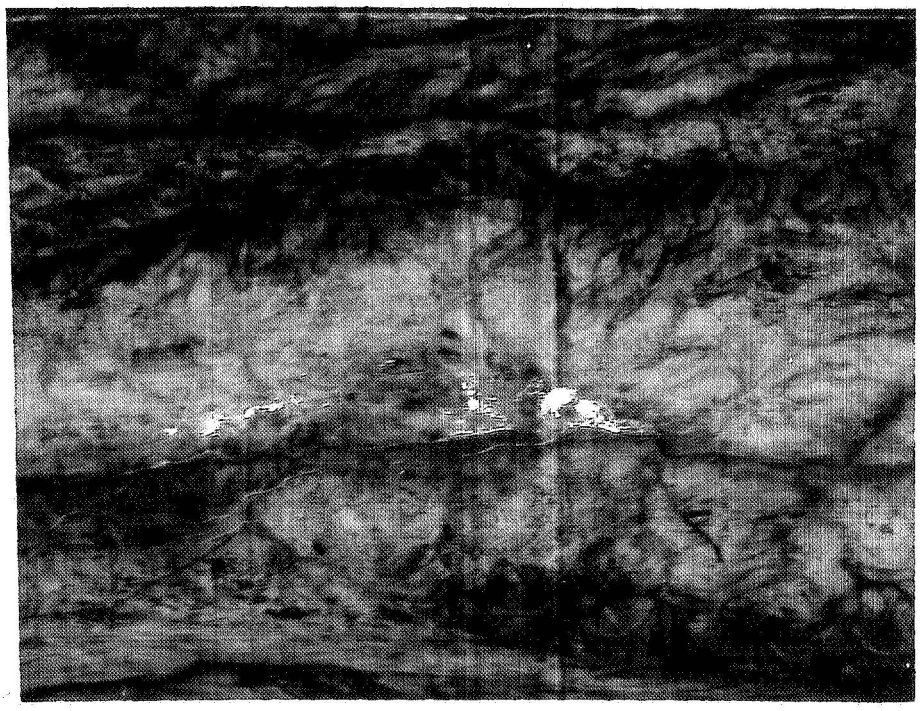

Figure 24. Aerial photos (bottom) and IR image (top) across the regional structure. Numerous areas show radiance as great as that in Big Sulphur Creek valley. For example, a brush covered slope (A) and several partly forested SW facing slopes (B,C) east of Squaw Creek. C=Cobb Creek; E=Big Sulphur Creek; F=Geyser Road; G=power plant no. 1. Letters on aerial photos correspond to those on infrared image.

FIG. 24

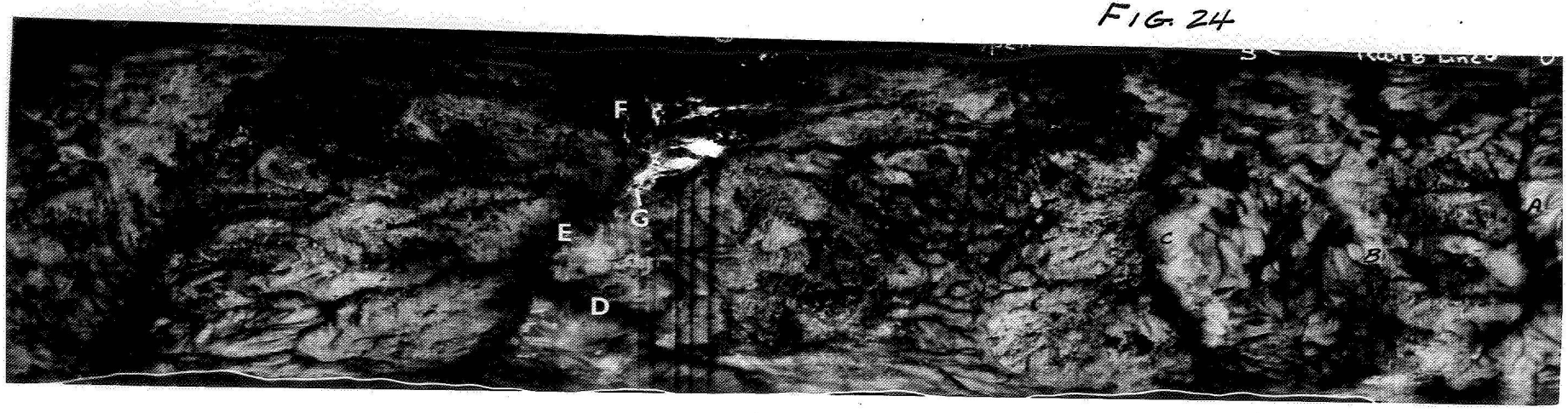

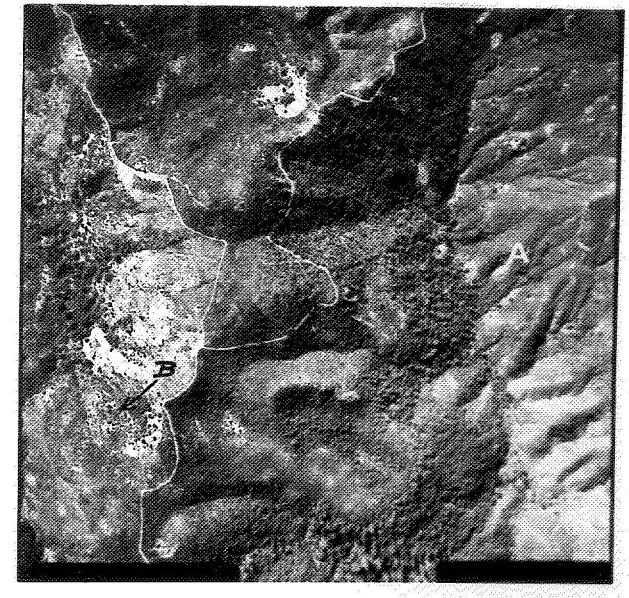

Figure 25. Aerial photos (bottom) and IR image (top) across the regional structure. Some apparent contradictions are illustrated. Barren area (A) and adjacent heavily forested area (B) west of the north branch of Little Sulphur Creek appear to have radiances reversed from similar barren area (C) and adjacent heavily forested area on the west slope of Big Sulphur Creek. E=Big Sulphur Creek; F=Geyser Road; G=Squaw Creek at the mouth of Cold Water Canyon; H=the Sulphur Banks. Arrows indicate position of arcuate radiance feature.

FIG 2.5